JOURNAL OF GEOPHYSICAL RESEARCH, VOL. 113, C02S20, doi:10.1029/2007JC004239, 2008

West Antarctic Peninsula sea ice in 2005: Extreme ice compaction and ice edge retreat due to strong anomaly with respect to climate

Robert A. Massom,[1] Sharon E. Stammerjohn,[2] Wouter Lefebvre,[3] Stephen A. Harangozo,[4] Neil Adams,[5] Theodore A. Scambos,[6] Michael J. Pook,[7] and Charles Fowler[8]

Received 20 March 2007; revised 31 August 2007; accepted 14 December 2007; published 19 February 2008.

[1] In September–October 2005, the juxtaposition of low- and high-pressure anomalies at 130°W and 60°W, respectively, created strong and persistent northerly airflow across the West Antarctic Peninsula (WAP). This had a major impact on regional sea ice conditions, with extreme ice compaction in the Bellingshausen and East Amundsen seas (60°W–130°W) but divergence in the West Amundsen and East Ross seas. This resulted in the former in a highly compact marginal ice zone and ice cover, mean modeled ice thicknesses of >5 m, and an earlier-than-average maximum extent (mid-August). While rapid ice retreat in late winter-spring created a major negative ice extent anomaly, compact ice persisted in the subsequent summer. Other effects were anomalies in air temperature (of +1°C to +5°C) and precipitation rates (to >2.5 mm/d). The patterns in late 2005 are consistent with the occurrence of a weak La Niña and a near-neutral Southern Annular Mode, with a quasi-stationary zonal wave three pattern dominating hemispheric atmospheric circulation. Once a compact ice edge was created, it took only one additional week of strong winds to "solidify" the pack in place. Conditions in 2005 are analyzed in the context of 1979–2005 and compared with the springs of 1993, 1997, 1999, 2001, and 2004. A statistically significant increase of the northerly 10-m wind component between 110°W and 125°W occurred in the Septembers of 1979–2005. No clear trends occur in other spring months. This work underlines the key importance of ice dynamics in recent changes in the WAP sea ice régime.

Citation: Massom, R. A., S. E. Stammerjohn, W. Lefebvre, S. A. Harangozo, N. Adams, T. A. Scambos, M. J. Pook, and C. Fowler (2008), West Antarctic Peninsula sea ice in 2005: Extreme ice compaction and ice edge retreat due to strong anomaly with respect to climate, *J. Geophys. Res.*, *113*, C02S20, doi:10.1029/2007JC004239.

1. Introduction

[2] Sea ice extent is a sensitive indicator of climate change/variability [*Intergovernmental Panel on Climate Change*, 2001], a fundamental measure of the area of ocean surface modified by an insulative and reflective sea ice cover [*Maykut*, 1986], and a key ecological parameter [*Ainley et al.*, 2003; *Brierley and Thomas*, 2002; *Loeb et al.*, 1997; *Nicol et al.*, 2000]. As such, gaining an improved understanding of mechanisms driving sea ice extent, and their spatiotemporal variability, is an essential prerequisite to an improved understanding of high-latitude change, ocean-atmosphere interaction and ecology, and the complex interactions and feedback processes involved. Nowhere is recent change more pronounced than in the West Antarctic Peninsula (WAP) region, which is under intense scrutiny as the only Antarctic sector to have experienced a significant warming trend over the past 50 years, i.e., of ~0.5°C per decade [*Vaughan et al.*, 2003], which has been linked to anthropogenic climate change. Of equal concern are concomitant environmental changes, including those in regional sea ice distribution, with major climatic and biological implications [*Fraser and Hofmann*, 2003; *Smith et al.*, 2003]. In fact, the WAP is also the only Antarctic sector to have experienced a statistically significant decreasing (negative) trend in sea ice extent since the 1970s [*Comiso*, 2003], primarily due to strong decreasing trends in spring-summer-autumn rather than winter [*Jacobs and Comiso*, 1997; *Smith and Stammerjohn*, 2001; *Stammerjohn and Smith*, 1997; *Zwally et al.*, 2002]. Also apparent is a negative trend in sea ice season annual duration [*Parkinson*, 2004]. While these changes have been attributed to the

[1]Australian Antarctic Division and Antarctic Climate and Ecosystems Cooperative Research Centre, Hobart, Tasmania, Australia.
[2]Lamont-Doherty Earth Observatory, Columbia University, Palisades, New York, USA.
[3]Institut d'Astronomie et de Géophysique Georges Lemaître, Université Catholique de Louvain, Ottignies-Louvain-la-Neuve, Belgium.
[4]British Antarctic Survey, Natural Environment Research Council, Cambridge, UK.
[5]Australian Bureau of Meteorology and Antarctic Climate and Ecosystems Cooperative Research Centre, Hobart, Tasmania, Australia.
[6]National Snow and Ice Data Center, University of Colorado, Boulder, Colorado, USA.
[7]CSIRO Division of Marine and Atmospheric Research, Hobart, Tasmania, Australia.
[8]Colorado Center for Astrodynamics Research, University of Colorado, Boulder, Colorado, USA.

warming trend in surface air temperature [*Smith et al.*, 2003; *Weatherly et al.*, 1991], recent papers show dynamic processes, i.e., wind-driven ice retreat, to be a major factor [*Jacobs and Comiso*, 1997; *Stammerjohn et al.*, 2003; *Massom et al.*, 2006; *Harangozo*, 2004a, 2006; *Harangozo and Connolley*, 2006].

[3] On seasonal to annual timescales, sea ice extent is determined by large-scale, climatological patterns of atmospheric and oceanic circulation and temperature. On shorter (e.g., synoptic) timescales, ice edge location changes rapidly in response to changes in wind direction associated with the passage of storms. While periods of ice retreat and subsequent advance during winter are not uncommon in the WAP region [*Harangozo*, 1997], sustained periods of retreat are rare. Only under unusual circumstances, for example, periods of sustained winds with a dominant meridional (northerly) component, do large-scale deviations in sea ice distribution persist over protracted periods of a few weeks and even months. One such atmospheric "event" occurred throughout the entire austral spring-summer of 2001–2002 to have a major impact on regional sea ice and associated biota [*Massom et al.*, 2006]. This was associated with the unusual persistence of deep low-pressure anomalies in the Bellingshausen and Weddell seas combined with a major high-pressure anomaly in the South Atlantic, as components of a quasi-stationary zonal wave three pattern in atmospheric circulation (see *Raphael* [2004, 2007] and *van Loon and Jenne* [1972] for more detailed information on this type of hemispheric pattern). It also entailed a strongly positive Southern Annular Mode (SAM) index. The SAM has been proposed as the dominant mode of variability in the pattern of atmospheric circulation around Antarctica (see *Simmonds and King* [2004] and the references therein for details). As such, it likely has a strong impact on Antarctic sea ice distribution and temperature [*Hall and Visbeck*, 2002; *Kwok and Comiso*, 2002a; *Liu et al.*, 2004; *Lefebvre et al.*, 2004].

[4] In this paper, we describe and analyze another major sea ice "compaction event" that occurred in the WAP region in late August through late November 2005 and left its mark through the subsequent summer, but was driven by a different atmospheric anomaly pattern. This entailed a rapid ice retreat in late winter-spring followed by the persistence of compact ice in the subsequent summer. The latter was among the warmest over the past 30 years, on the basis data from six weather stations in the region [*Skvarca et al.*, 2006]. The atmospheric anomaly responsible appeared not to be associated with a strong phase of SAM (unlike the 2001–2002 anomaly just described) but may have been influenced by a La Niña event. There is considerable evidence for strong El Niño–Southern Oscillation (ENSO) teleconnections in the South Pacific atmospheric circulation [*Karoly*, 1989; *Kiladis and Mo*, 1998; *Harangozo*, 2000, 2004b; *Raphael*, 2003; *Vera et al.*, 2004; *Lachlan-Cope and Connolley*, 2006] and sea ice extent [*Harangozo*, 2000; *Yuan and Martinson*, 2001; *Kwok and Comiso*, 2002b; *Renwick*, 2002; *Stammerjohn et al.*, 2003]. On average, during El Niño events, when the central Pacific warms and deep tropical convection is widespread, atmospheric blocking and ridging increase in the WAP and Bellingshausen Sea in austral winter and spring. The associated cold southerly winds produce above-normal ice extent here. Farther to the west in the western Amundsen Sea and eastern Ross Sea, northerly winds increase during El Niño events, resulting in lower ice extent than normal. During La Niña events, reverse circulation and sea ice anomalies occur on average. *Yuan and Martinson* [2001] have termed the ENSO-related dipole pattern of contrasting ice anomalies in the Weddell Sea and eastern South Pacific the "Antarctic Dipole."

[5] Here we analyze atmospheric and associated sea ice conditions in 2005, in the context of the period 1980–2005 and compared to both the 2001/2002 event and another unusual winter ice retreat in 1993 (reported by *Turner et al.* [2002]). Further comparison is made with conditions in 1997, 1999 and 2004 (a more typical year). We examine the impact not only on sea ice extent but also on ice concentration, ice thickness, snowfall, the nature of the marginal ice zone, air temperature, precipitation rate and ship navigation in the WAP region. We also evaluate the relative role of short-term versus more sustained wind-forcing events, and the important impact on sea ice conditions during the subsequent summer (melt) period.

2. Data and Techniques

[6] The atypical sea ice distributions in late 2005 were initially discovered in daily ice concentration maps derived in near real-time from NASA Aqua Advanced Microwave Scanning Radiometer-EOS (AMSR-E) data using the ARTIST Sea Ice (ASI) algorithm [*Kern and Clausi*, 2003]. These maps, at a spatial resolution of 6.25 km, were obtained from the University of Bremen (see www.seaice.de). Longer-term analysis was carried out using monthly mean sea ice concentrations derived from the combined Defense Meteorological Satellite Program (DMSP) Special Sensor Microwave/Imager (SSM/I, 1987 to the present) and Nimbus 7 Scanning Multichannel Microwave Radiometer (SMMR, 1978–1987), using the NASA Bootstrap algorithm [*Comiso*, 1995, 2005]. These data (obtained from the US National Snow and Ice Data Center [NSIDC]) are gridded with a pixel size of 25 × 25 km. Information on the timing of sea ice retreat for each year and each pixel was derived from daily sea ice concentration data. The final day of sea ice is when the concentration decreases below 15% (i.e., the approximate ice edge) and remains below 15% until the end of the annual search window (which is mid-February to mid-February, i.e., the mean summer sea ice extent minimum). More detailed information on sea ice morphology and ice edge configuration was derived from higher resolution (0.25 km) visible images from the NASA Moderate Imaging Spectroradiometer (MODIS), obtained from NASA's Distributed Active Archive Center. The analysis also included maps of monthly averaged ice motion derived from SSM/I satellite data, obtained from the NSIDC Polar Pathfinder database [*Fowler*, 2003] using the technique described by *Emery et al.* [1995].

[7] Information on the large-scale atmospheric patterns responsible for the observed sea ice anomalies, and associated wind, temperature and precipitation fields, was derived from mean sea level pressure (MSLP) and 500-hPa geopotential height data from the National Centers for Environmental Prediction/National Center for Atmospheric Research (NCEP/NCAR) Reanalysis 2 project (henceforth referred to as NNR2) [*Kalnay et al.*, 1996]. Wind velocity data were computed from 10-m zonal and meridional

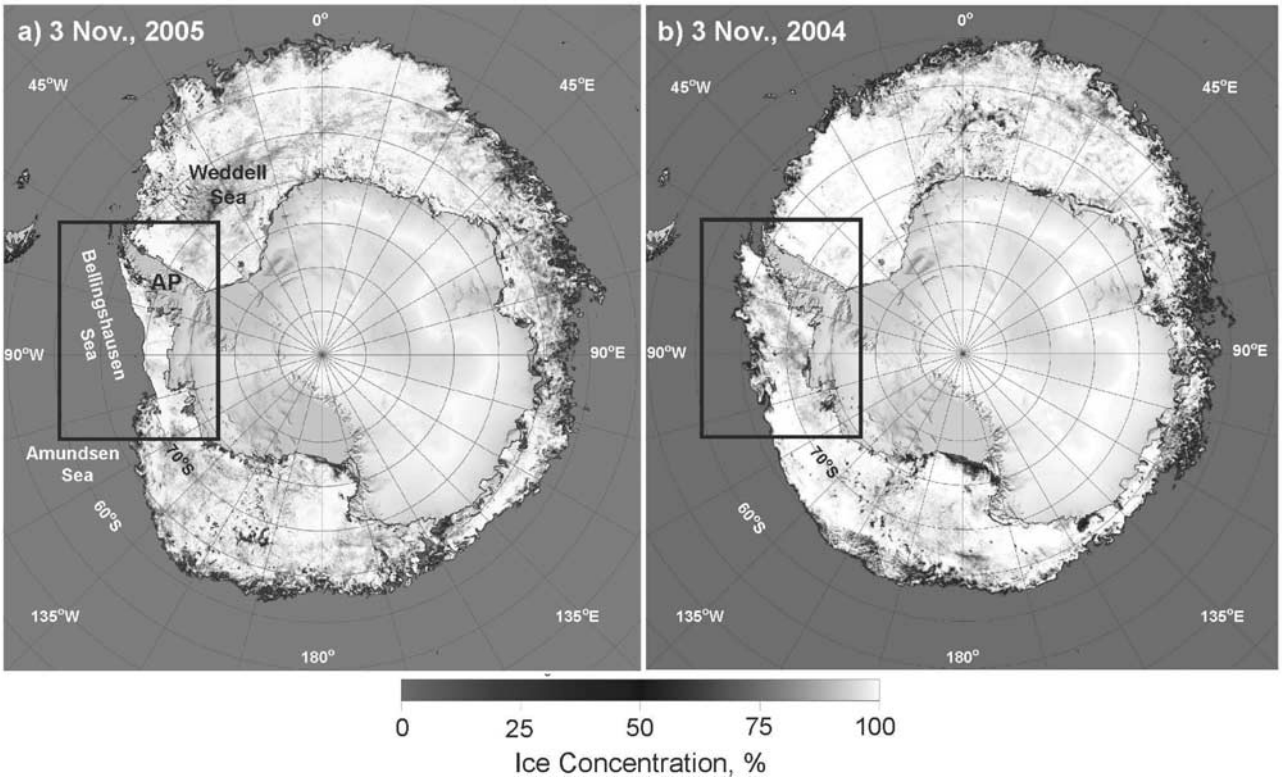

Figure 1. Maps of daily Antarctic sea ice concentration for (a) 3 November 2005 and (b) 3 November 2004, derived from NASA Aqua AMSR-E data.

monthly mean winds from the NNR2 data set. These data are in equal-area format, with a grid size of ~1.89° (meridional) by 1.875° (zonal). For comparison, data were also acquired from the European Centre for Medium Range Weather Forecasting (ECMWF) Re-Analysis (ERA-40) project [*Uppala et al.*, 2005].

[8] Monthly wind field anomalies were computed using monthly means for the period 1980–2005. No NNR2 data are used before 1979 owing to their unreliability prior to this date [*Hines et al.*, 2000; *Marshall and Harangozo*, 2000]. Meteorological data collected at Rothera Station in Marguerite Bay (WMO ID 89062, 67.51°S, 68.1°W) were used to verify patterns observed in the NNR2 analysis. Information on the monthly SAM index, derived using the algorithm of *Marshall* [2003], was obtained from the British Antarctic Survey at: http://www.nerc-bas.ac.uk/icd/gjma/sam.html. Southern Oscillation Index values were obtained from the NOAA (National Oceanic and Atmospheric Administration) Climate Diagnostics Center (http://www.cdc.noaa.gov/ENSO/enso.current.html#indices).

[9] Given the lack of contemporary in situ measurements, the impact of the atmospheric circulation in late 2005 on sea ice thickness is modeled. The model used, called ORCALIM, results from the coupling of the Louvain-la-Neuve sea ice model (LIM) [*Fichefet and Morales-Maqueda*, 1997] with the hydrostatic primitive equation model OPA (Océan PArallélisé) [*Madec et al.*, 1999]. The coupling technique between OPA and LIM is identical to the one described by *Goosse and Fichefet* [1999]. The model version used here is the same as that used by *Timmermann et al.* [2005], which includes a more detailed model description and a validation of the model.

3. Anomalous Atmospheric Circulation and Sea Ice Distributions in Late 2005 to Early 2006

[10] Comparative AMSR-E images of Antarctic sea ice concentration and extent from early November in 2005 and 2004 are shown in Figure 1. Immediately striking is the extraordinary compactness of the marginal ice zone in the Bellingshausen and East Amundsen seas sector (from 60°W to 105°W) in 2005, both compared to the remaining circumpolar pack and the same region in 2004. Here the sea ice edge zone is extremely well defined compared to the more typical diffuse marginal ice zone in other regions and at other times. Indeed, the RRS *James Clark Ross* was delayed by 2 days getting into Rothera Station in December 2005 owing to unusually heavy ice conditions, with few leads and large thick floes remaining intact by being blown against the coast.

[11] This pattern is indicative of wind-driven compaction of sea ice against the WAP over an extended period, as confirmed by examination of NNR2 surface wind anomaly fields (monthly mean, with respect to 1980–2006) superimposed on monthly mean SSM/I-derived ice concentration maps for October and November 2005 (Figures 2b and 2c). Long-term mean locations (1980–2001) of the 15% and 75% ice concentration contours are marked as black dotted and black dashed lines, respectively. Comparison with the monthly mean 15% and 75% ice concentration contours

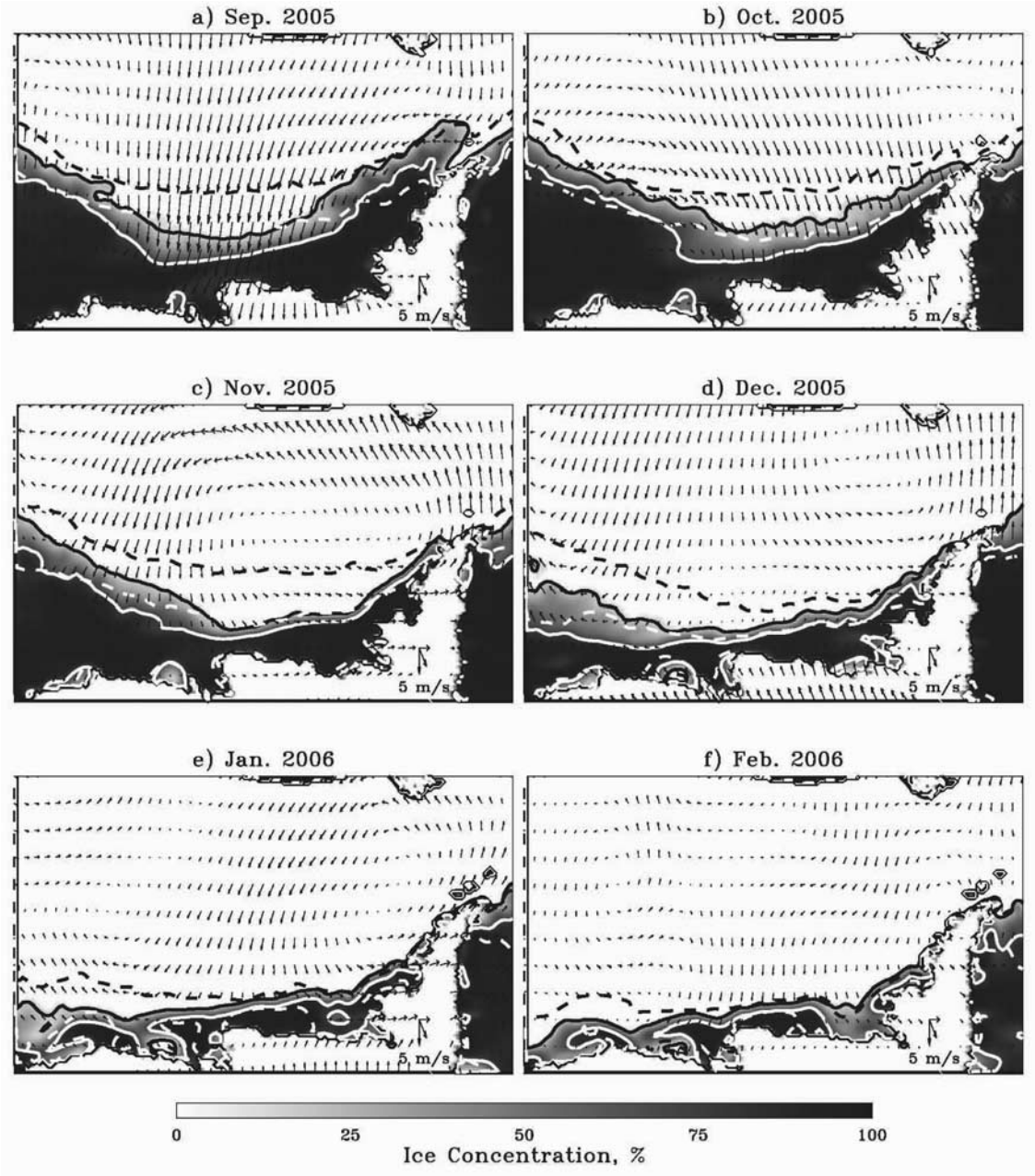

Figure 2. Monthly mean NNR2 surface wind field anomaly vectors (based on 1980–2006) superimposed on monthly mean SSM/I-derived ice concentration maps for (a) September 2005, (b) October 2005, (c) November 2005, (d) December 2005, (e) January 2006, and (f) February 2006. Long-term mean locations (1980–2001) of the 15% and 75% ice concentration contours are marked as black dotted and black dashed lines, respectively, and monthly mean 15% and 75% ice concentration contours are white and black lines respectively.

(white and black lines, respectively) shows that a major ice-edge recession (negative ice extent anomaly) occurred toward the Peninsula in late winter-spring 2005, with an increase in ice concentration. A further striking feature is the unusually narrow transition from open ocean to consolidated pack at the ice edge. These are due predominantly to dynamically driven ice compaction by the persistent strong winds with a dominant northerly-northwesterly component. The dominance of strong winds blowing ice against the peninsula is further indicated by the modeled wind stress and wind stress anomaly maps for late October to early November 2005 (not shown).

[12] The large-scale atmospheric circulation patterns responsible are shown in Figure 3, a map of mean composite anomalies in 500-hPa geopotential height for the Southern Ocean and Antarctica for September–October 2005 (compared to the September–October mean of 1980–2005). Standout features are a strong negative anomaly of <-75 m centered

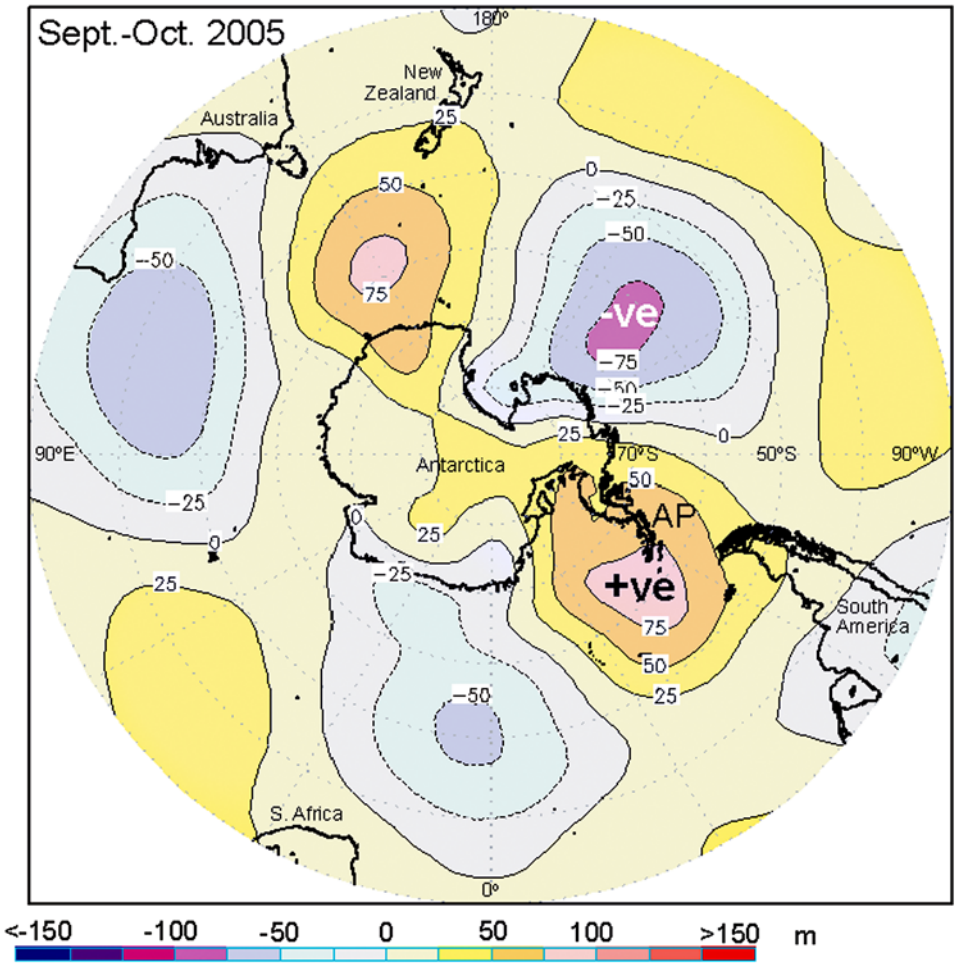

Figure 3. Map of mean composite anomalies in 500-hPa geopotential height for the Southern Ocean and Antarctica for September–October 2005 (compared to the September–October mean of 1980–2005). Here −ve and +ve denote the low- and high-pressure anomalies respectively, and AP is Antarctic Peninsula.

on the Amundsen Sea, and an equally strong positive anomaly (>75 m) in the NW Weddell Sea. These anomalies combined indicate the sustained channeling of winds with a dominant northerly component into the WAP sector (60°W–105°W), and a concomitant outflow of cold air from the continent in the vicinity of 105°W–140°W. On the hemispheric scale, the configuration of alternate positive and negative centers resembles a quasi-stationary zonal wave three pattern in atmospheric circulation [*Raphael*, 2004, 2007; *van Loon and Jenne*, 1972]. How this atmospheric anomaly pattern compares to the high-latitude response to SAM and/or ENSO will be discussed in section 4.

[13] The impact of this atmospheric circulation on the regional wind field and sea ice cover is apparent in 250-m resolution MODIS channel 2 (0.841–0.876 μm) image from 3 November 2005 in Figure 4a. This confirms the extreme sea ice compaction observed in the AMSR-E data (Figure 1a). As noted with Figure 2, the transition from open ocean to consolidated pack is unusually narrow over a wide zone, with an extraordinary clarity in the ice edge. The resultant compact nature of the marginal ice zone (MIZ) is shown in detail in Figure 4b. The dashed line separating the MIZ from the inner pack demarcates the approximate location of a significant change in surface reflectance in the MODIS data. This relates to the change in surface characteristics (floe size, surface wetting, snow thickness) with distance from the ice edge in response to the damping of ocean swell propagating through the pack. Such a damping of wave energy occurs over a shorter distance in high- compared to low-concentration ice [*Squire et al.*, 1995].

[14] Examination of the satellite imagery shows that the unusual pattern of extreme wind-driven dynamic compaction and ice edge recession affected the sea ice zone of the entire Bellingshausen Sea and the eastern part of the Amundsen Sea, from ~60° to 105°W, equivalent to a continuous ice edge front >2200 km long. It first formed in late August 2005, became well developed by mid-September and persisted through late November 2005, with a brief synoptic-scale reversal or ice divergence event in early October (Figure 5). Under more normal circumstances related to the passage of storms, periods of ice edge compaction are limited to episodes of on-ice winds lasting

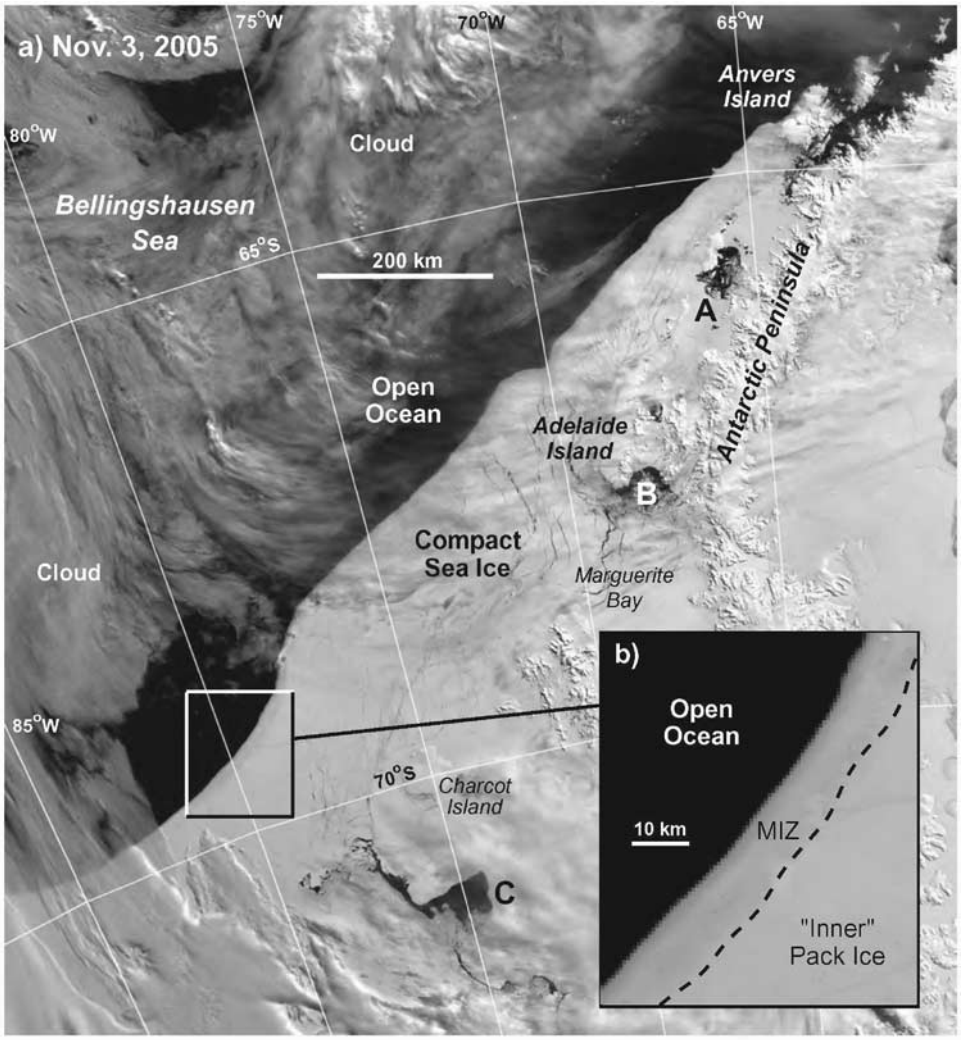

Figure 4. (a) A 250-m resolution MODIS channel 2 (0.841–0.876 μm) image of sea ice in the WAP region, 3 November 2005. (b) Inset showing a magnification of the region within the box.

a matter of days at any one time (rather than for weeks, as was the case in 2005).

[15] Monthly mean maps of SSM/I-derived ice motion for September–December 2005 are shown in Figure 6. Ice drift agrees well with the wind anomalies shown in Figure 2. An outstanding feature of the September to November maps is the zone of very low ice drift velocities in the approximate sector 60°W–110°/120°W. This mirrors the relative lack of motion as a result of compaction against the peninsula forced by winds with a dominant northerly component.

[16] The regional significance of this wind-driven sea ice anomaly is further illustrated in Figure 7, a comparison of monthly mean ice concentration anomaly maps for August–November 2005 with MSLP anomalies overlain. These were produced by subtracting monthly SSM/I-derived ice concentration values from mean values for the months in question over the period 1980–2005. An anomaly was calculated only where there was sea ice for the year/month in question (e.g., August 2005), thereby reflecting the actual ice edge for the period in question. The Amundsen-Bellingshausen Sea sector switches from above-average concentrations (extent) in August 2005 to strong negative anomalies in September through November 2005. These are accompanied by positive anomalies against the coast, as expected in a wind-driven ice compaction scenario. They are to some extent balanced by positive sea ice concentration and extent anomalies elsewhere, for example, in the Ross Sea, which is associated with the outflow of continental air along the western limb of the Amundsen Sea negative pressure anomaly. In fact, the total extent anomalies for the entire Antarctic sea ice cover for August through November 2005 are minimal, at -0.1, 0.4, 0.1 and 0.2 $\times$ 10^6 km^2, respectively. The regional differences are not, however.

[17] The ice concentration anomaly patterns in Figure 7 illustrate the classic Antarctic Dipole [*Yuan and Martinson*, 2001]. The August [2005] pattern resembles the El Niño response (with high pressure centered on $\sim$130°W), whereas the October case resembles the La Niña response (with low pressure centered on $\sim$130°W). The Southern Oscillation Index (SOI) values indeed switch from a negative SOI in August (-1.3) to a negative value in October (+1.9). This

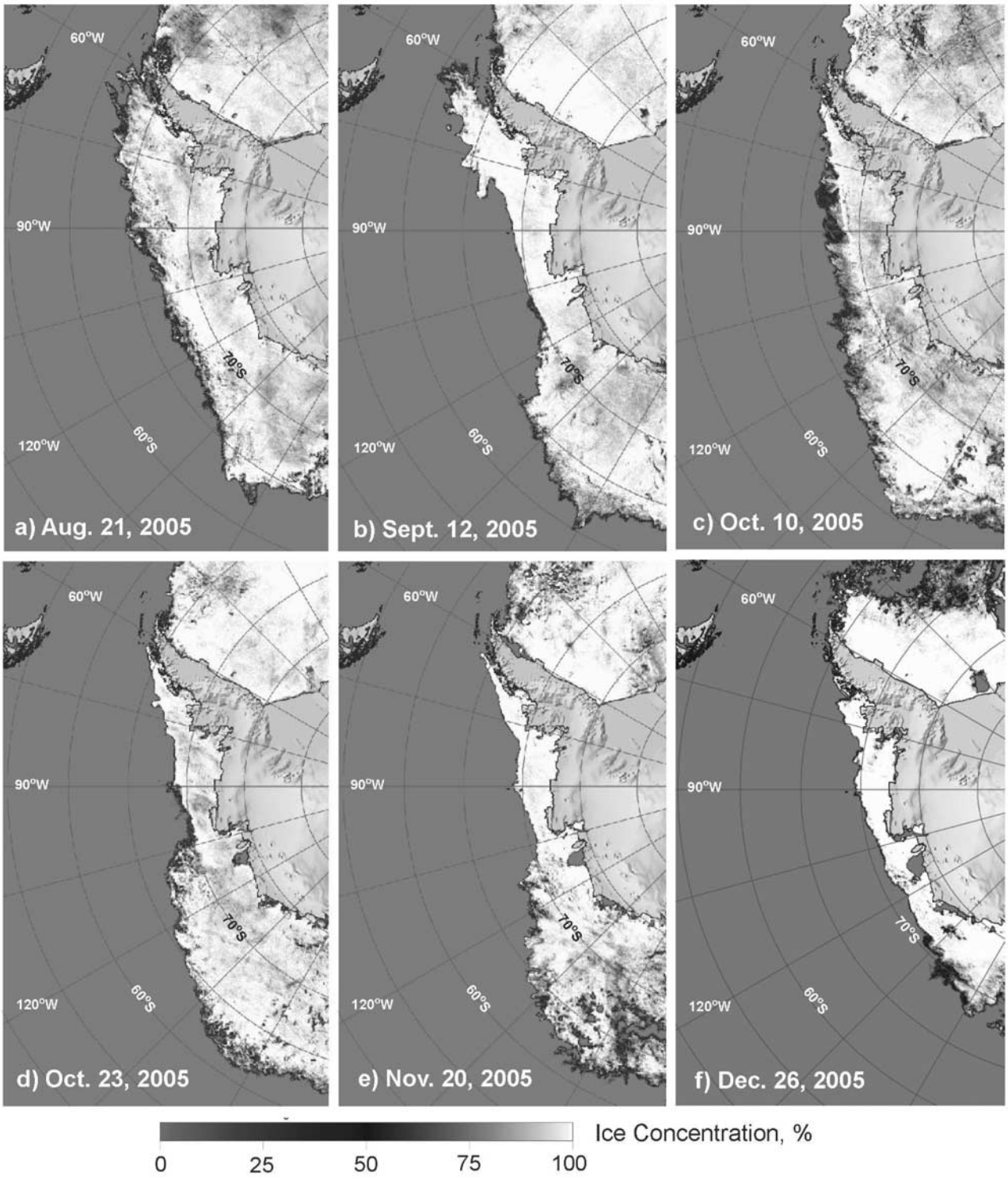

Figure 5. Daily AMSR-E sea ice concentration images (resolution 6.25 km) from (a) 21 August, (b) 12 September, (c) 10 October, (d) 23 October, (e) 20 November and (f) 26 December (all 2005), showing the development of the extraordinary ice edge recession and compaction in late 2005.

is a further illustration, following on from *Harangozo* [2000] and *Stammerjohn et al.* [2003], of how quickly (1) the high-latitude atmosphere responds to tropical SOI/ENSO anomalies, and (2) the marginal ice zone adjusts to the overlying atmospheric condition.

[18] The impact on the magnitude and temporal aspects of regional ice extent is shown in Figure 8, which compares time series of ice extent in the sector 60°W–100°W for the periods August to late December for 2005 (Figure 8a) and 2004 (a more typical year) (Figure 8b). In 2005, the mid-August to early-September period (marked A) is character-

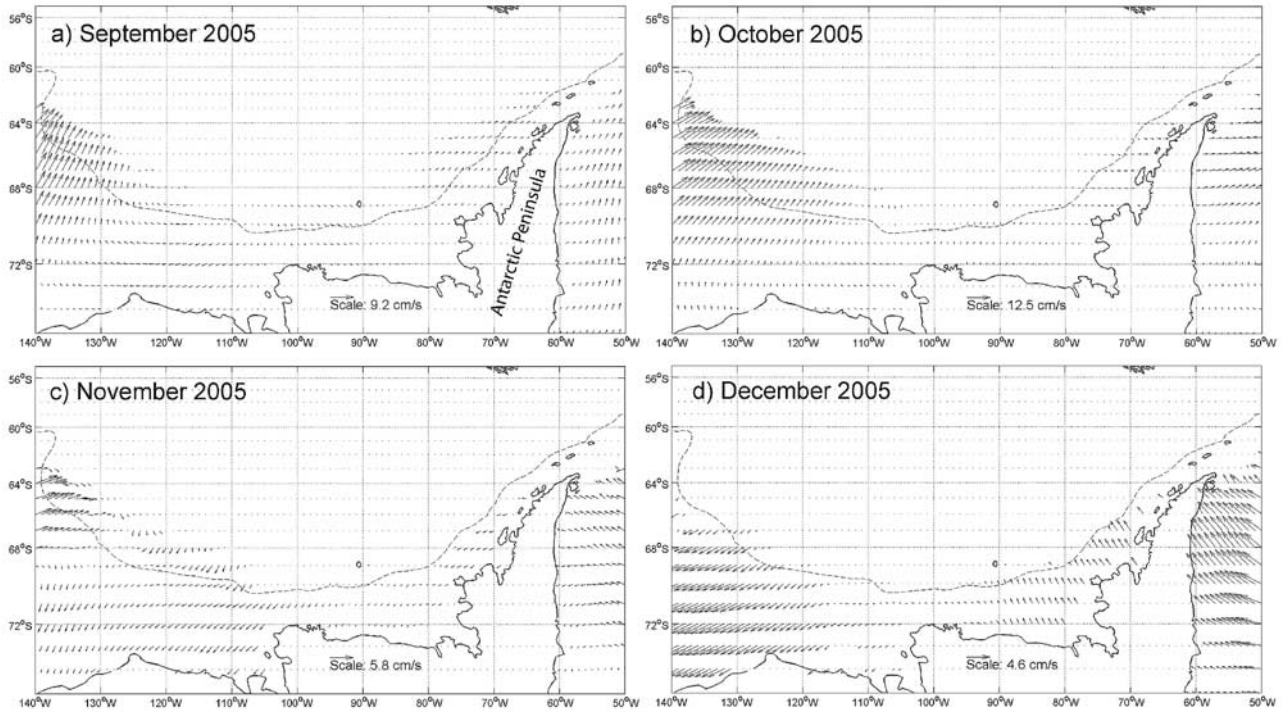

Figure 6. Monthly mean ice motion maps for (a) September, (b) October, (c) November, and (d) December 2005, derived from SSM/I data. Data obtained from the NSIDC Polar Pathfinder Program. The dashed line is the approximate location of the Southern Boundary of the Antarctic Circumpolar Current [*Orsi et al.*, 1995].

ized by a major decrease in ice extent in the sector, of ~46% in 3 weeks, followed by some fluctuation (two temporary reversals) over the subsequent 5–6 weeks (marked B and C). In contrast, the sector in 2004 experiences a major build-up in the early-August to late-September timeframe, of ~60% in 6 weeks (marked E). This is followed by a steady and fairly consistent decrease over a much longer period (marked F) than in 2005, then a lower rate of decrease in period G. In 2005, the rapid decrease and fluctuation phases are followed by a flattening (quasi-stabilization) of the ice extent (phase D), in this case signifying resistance of the ice to further dynamic compaction against the Peninsula. Owing to these differences, maximum ice extent occurs in mid-August in 2005, compared to late September in 2004. Phases F and G occurred earlier in 2005, reaching a low extent plateau in late October (versus late December in 2004).

4. Discussion

[19] The results presented here suggest that the negative spring ice extent anomaly and compaction in the WAP sector in 2005 was driven by sustained strong winds with a dominant meridional (northerly) component, associated with a quasi-stationary (standing) zonal wave three pattern (as shown in Figure 3). This is consistent with the findings of *Lefebvre and Goosse* [2008], in their longer-term analysis of atmospheric processes driving large-scale interannual variability in Antarctic winter sea ice. Regional sea ice behavior in late 2005 is also consistent with the occurrence of a weak La Niña event, i.e., a positive SOI value, as noted above, with a tendency for a low MSLP anomaly in the Amundsen Sea. At such times, there is a tendency for less ice in the Antarctic Peninsula region [e.g., *Kwok and Comiso*, 2002b; *Yuan and Martinson*, 2001; *Harangozo*, 2000; *Stammerjohn and Smith*, 1996]. Intense and persistent northerly airflow across the WAP region (from ~130°W to the tip of the peninsula) in September–October 2005 resulted from the juxtaposition of a low MSLP anomaly at 130°W and a high MSLP anomaly at 60°W. This compacted ice against the coast (i.e., caused ice convergence) in the Bellingshausen and eastern Amundsen seas, while blowing ice offshore (i.e., created divergence) in the western Amundsen and eastern Ross seas.

[20] In recent decades, the SAM has assumed an increasingly positive polarity [*Simmonds and Keay*, 2000; *Thompson et al.*, 2000], leading to a strengthening of the westerly wind field [*Liu et al.*, 2004]. The atmospheric circulation in late 2005 appears not to conform to this trend. The SAM Index values converge toward zero at this time, and exhibit the weakest combined signal in the entire 25-year record (for August–November data) shown in Figure 9. The monthly mean SAM Index fluctuated from positive to negative and back, with monthly values of 0.50, 0.39, −0.11 and 0.66 from August through November 2005, respectively (Figure 9a). The signal was stronger in the concomitant SOI, with values of −1.3, +0.7, +1.9 and −0.5 (Figure 9b). The October value in particular (of +1.9) is amongst the highest in the 25-year time series, and compares with an October average of 0.53. Being neutral, the SAM was neither reinforced nor neutralized by the ENSO

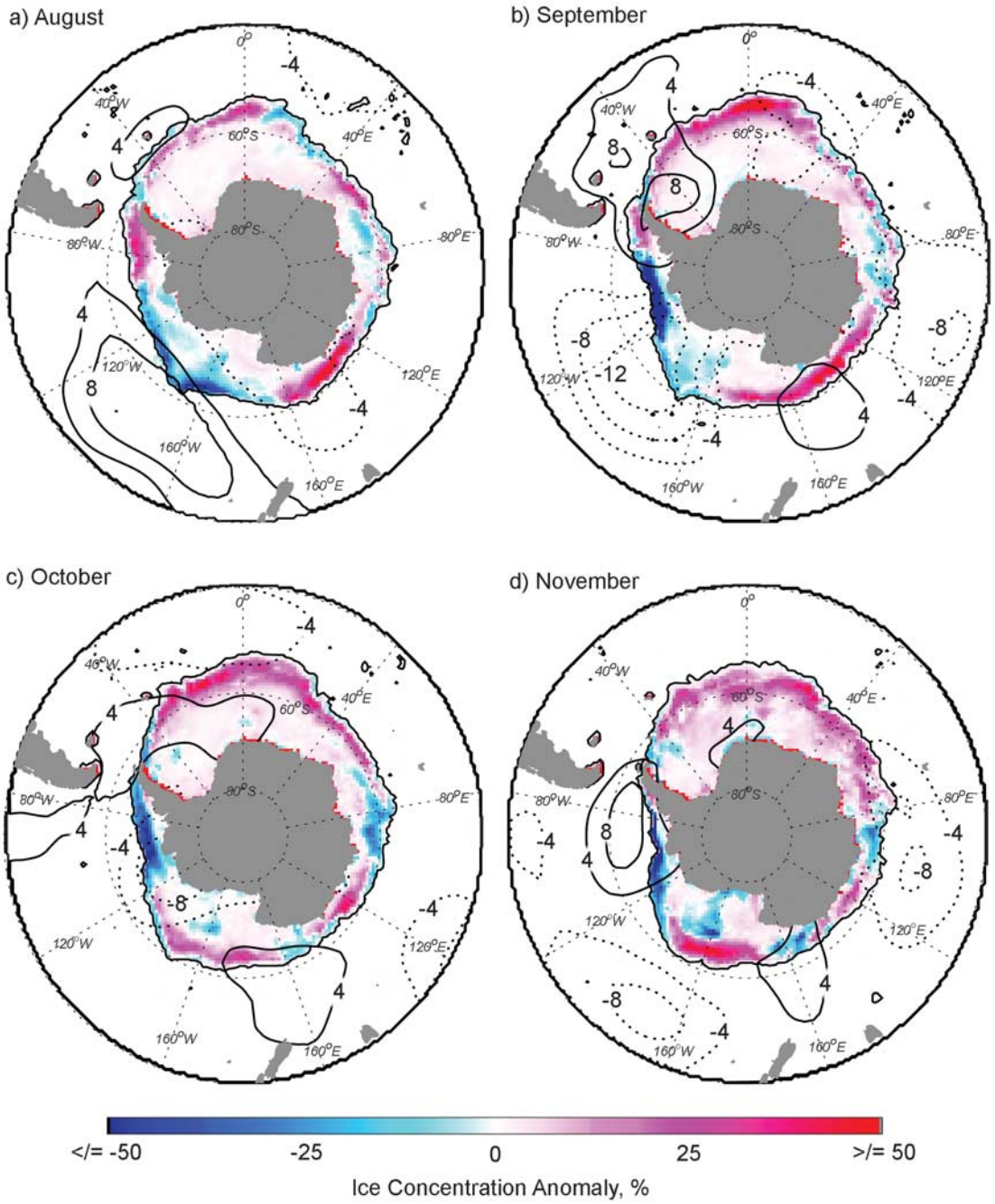

Figure 7. Monthly mean ice concentration anomaly maps for (a) August, (b) September, (c) October, and (d) November 2005, compared to the monthly means for 1979–2000, with MSLP anomaly overlay (in hPa).

response, an observation we explore and discuss further in section 4.3. Rather, the quasi-stationary zonal wave three pattern dominates the hemispheric atmospheric circulation.

4.1. Impact in 2005

[21] Near-surface monthly mean meteorological (NNR2) data for September from ~69.5°S, 90.0°W and for the period 1979–2005 (Figure 10) illustrate the impact of the anomalous atmospheric circulation pattern in the WAP region. This point was chosen as it falls approximately halfway along the compact ice "front" in Figure 5. Key findings are as follows.

[22] 1. The monthly mean wind speed for September was the highest on record at 7.5 m s^{-1} (since 1954), and from the NNE (28°). This compares to a 1980–2005 mean of 3.1 ± 1.9 m s^{-1}, with September winds typically varying between southeasterly and northwesterly (through west). There are occasional years of north-northeasterly winds in

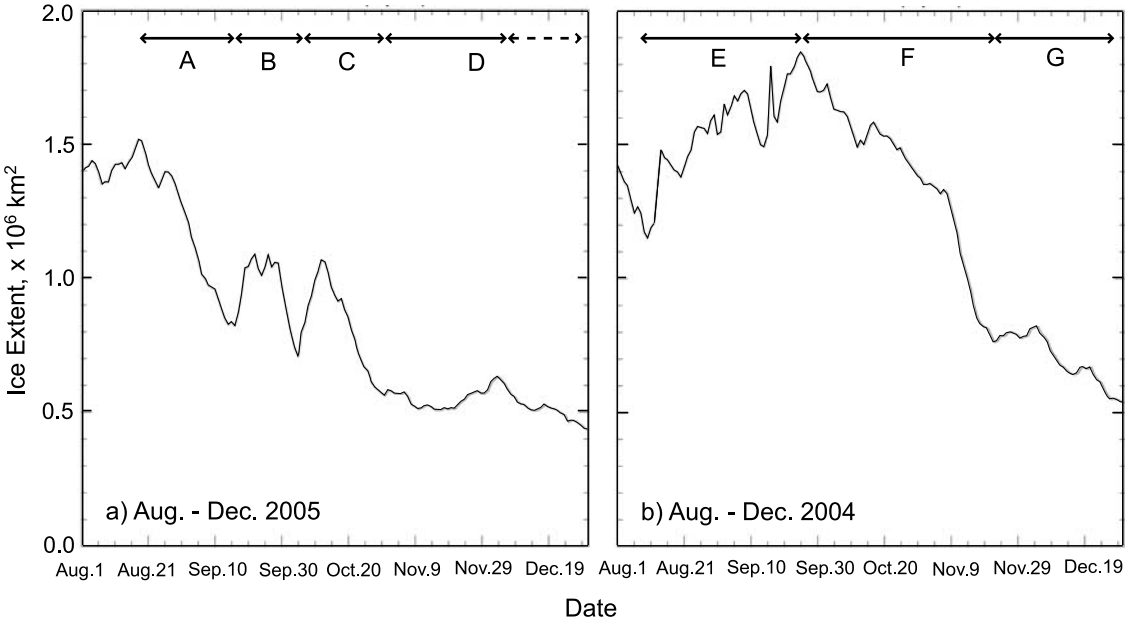

Figure 8. Plots of daily mean ice extent in the sector 60°W–100°W for the periods August to late December for (a) 2005 and (b) 2004 (a more typical year). Each minor tick represents 5 days. Please see text for an explanation of labels A-G.

September but these tend to be light, i.e., <3 m s^{-1}. The combined ECMWF operational and ERA-40 record (not shown) indicates that the monthly average northerly wind component at 90°W, 69.5°S was the strongest on record in September and October 2005.

[23] 2. The monthly mean September MSLP pattern is dominated by a very strong low (969 hPa in the mean) centered near 69°S, 126°W, just ''upstream'' from the anomalous ice area. This gave a strong southward push to ice drift in the area of interest.

[24] 3. The mean September 2-m air temperature of −4.1°C is the second highest in the 1980–2005 record (behind −3.9°C in 2002). By comparison, the lowest temperature occurred in 1984 (−24.7°C), and the 1979–2005 mean is −15.2 ± 5.0°C.

[25] 4. The mean monthly specific humidity reached 2.8 g kg^{-1}, again just behind the record value of 2.9 g kg^{-1} for 2002. The associated precipitation rate of 4.2 mm d^{-1} is by far the largest on record. The long-term mean at this location is 2.1 ± 0.8 mm d^{-1}.

[26] A strong feature of the time series in Figure 10 is a trend in mean September 2-m air temperature, specific humidity and precipitation rate and near-surface wind speed from about 1990 onward. This is closely allied to an apparent switch in the extremes of mean wind direction from the SSE-W sector to more northerly-northwesterly (although southwesterly winds dominate in some years, i.e., 1992–1994 and 2003–2004). More northerly winds would advect warmer, moister air across the WAP sea ice zone and the Peninsula itself. In general, the highest speeds are associated with winds with a more northerly component. A switch in mean wind direction could also be due to changes in SAM, due to the deep low-pressure anomaly in the Amundsen Sea in high SAM years [e.g., *Lefebvre et al.*, 2004]. In fact, other work has highlighted a switch in SAM from a more negative state in the 1980s to a more positive state in the 1990s [*Stammerjohn et al.*, 2008; *Thompson and Solomon*, 2002]. Linear regression analysis of the Figure 10 time series from 1990 to 2005 yields per annum increases of ∼0.20 m s^{-1} in wind speed, ∼0.63°C in 2-m air temperature, ∼0.06 g kg^{-1} in specific humidity, and ∼0.10 mm d^{-1} in precipitation.

[27] The magnitude of the temperature trend in Figure 10 is larger than expected. At ∼6.3°C per decade, it is an order of magnitude greater than the approximately 0.5°C per decade reported previously from station records [e.g., *King and Harangozo*, 1998]. This prompted (1) a comparison with ERA-40 data from roughly the same location (70.0°S, 90.0°W) and (2) a comparison of in situ observations at Rothera Base with NNR2 and ERA-40 data from model grid cells closest to the base, all over the period 1980–2005 (September means). At Rothera, the ERA-40 data largely replicate the observations by displaying no apparent trend, while the NNR2 data set displays similar trends to those in Figure 10. Clearly, this apparent discrepancy between NNR2 and ERA-40 requires further investigation (beyond the scope of this paper). However, the ERA-40 record at 70.0°S, 90.0°W is similar to the NNR2 record in Figure 10, in that there are positive trends in near-surface air temperature and relative humidity. In fact, these are physically plausible in that they are associated with a concomitant change in wind direction to a more northerly to northwesterly component. This is consistent with the apparent change of the SAM from a more negative to more positive state in the 1990s [*Lefebvre et al.*, 2004; *Thompson and Solomon*, 2002], and the prevalence of coincident La Niña events [*Stammerjohn et al.*, 2008].

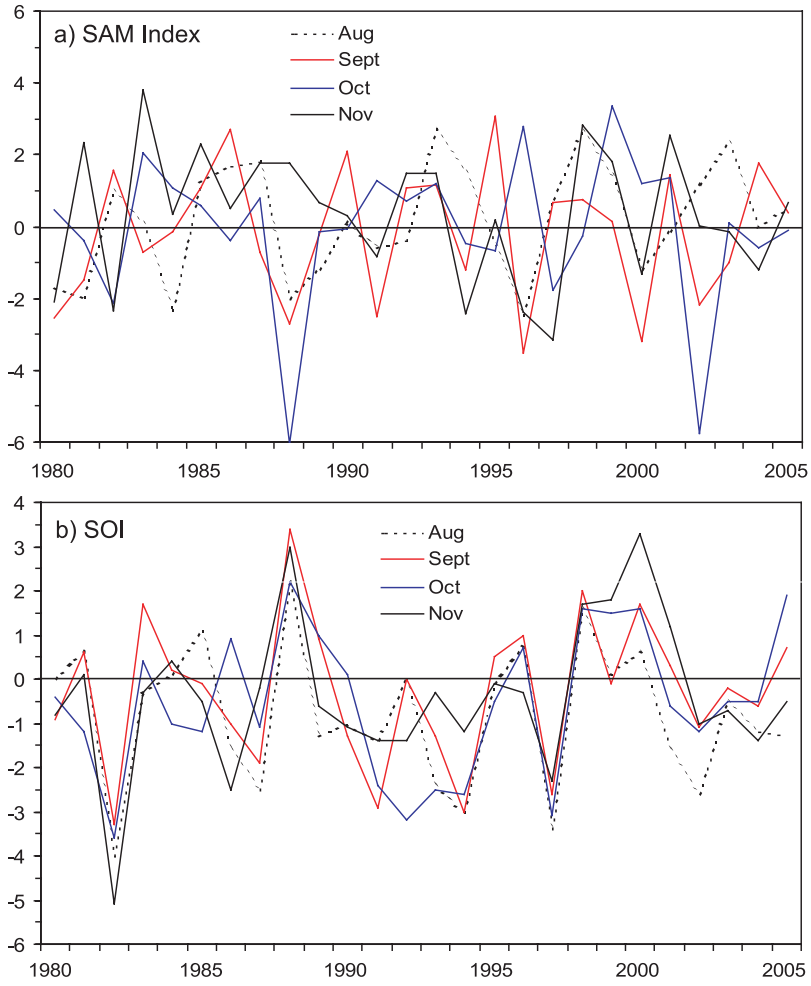

Figure 9. Time series of (a) the SAM Index and (b) the Southern Oscillation Index (SOI) for the months August, September, October, and November, 1980–2005.

[28] Figure 11 casts some light on this, by depicting the trend in the September combined 10 m meridional (V component) wind record extracted from the ECMWF 40 year reanalysis up to 2001 and thereafter from the ECMWF operational analyses. This shows that in September there has been a long-term increase in northerly winds in the western part of the region of retreat in 2005. In particular, there has been a statistically significant increase of the northerly wind component around 110°W–125°W that reaches well into the spring sea ice zone to about 71.5°S. It is also interesting that the greatest ice retreat during September 2005 occurred in the western and central Bellingshausen Sea rather than around the WAP coast (not shown). Figure 7b confirms that pronounced negative sea ice concentration anomalies first developed in this part of the study area in the 2005 spring. It was only in October 2005 that negative anomalies became established in the WAP. This eastward spreading of negative ice concentration anomalies between September and October is consistent with the strongest northerly wind anomalies moving eastward over these two months (Figure 2).

[29] The overall impact of conditions in late 2005 on near-surface (2 m) air temperature and precipitation rate is illustrated in regional anomaly maps for October 2005 (Figure 12). These are derived by subtracting the average values of all Octobers from 1979 to 2005 from the mean monthly (October) fields in 2005. Standout features are a) a band of higher air temperatures along the Amundsen-Bellingshausen (AB) region and across almost the entire Weddell Sea, and b) a major precipitation rate anomaly across the AB region. In fact, the entire AB region is enveloped by an air temperature anomaly that ranges from +1°C in the north to +5°C in the southwest. Values of >+7°C occur in the central Weddell Sea. The associated precipitation rate anomaly also extends the length of the WAP region, with centers of >2.5 and >2 mm/d in the East Amundsen/West Bellingshausen seas and NE Bellingshausen Sea, respectively.

[30] As in 2001 [*Massom et al.*, 2006], the dominance of a relatively warm northerly airstream in September–November 2005 is confirmed by Rothera observations. The mean September–October–November (SON) air temperatures in 2005 were −6.6 ± 5.5°C, −3.3 ± 4.1°C and −1.1 ± 2.3°C, respectively. These compare to long-term mean SON temperatures (for 1980–2005) of −8.6 ± 6.9°C, −5.5 ± 4.9°C and −2.1 ± 3.0°C. Higher air temperatures can have a

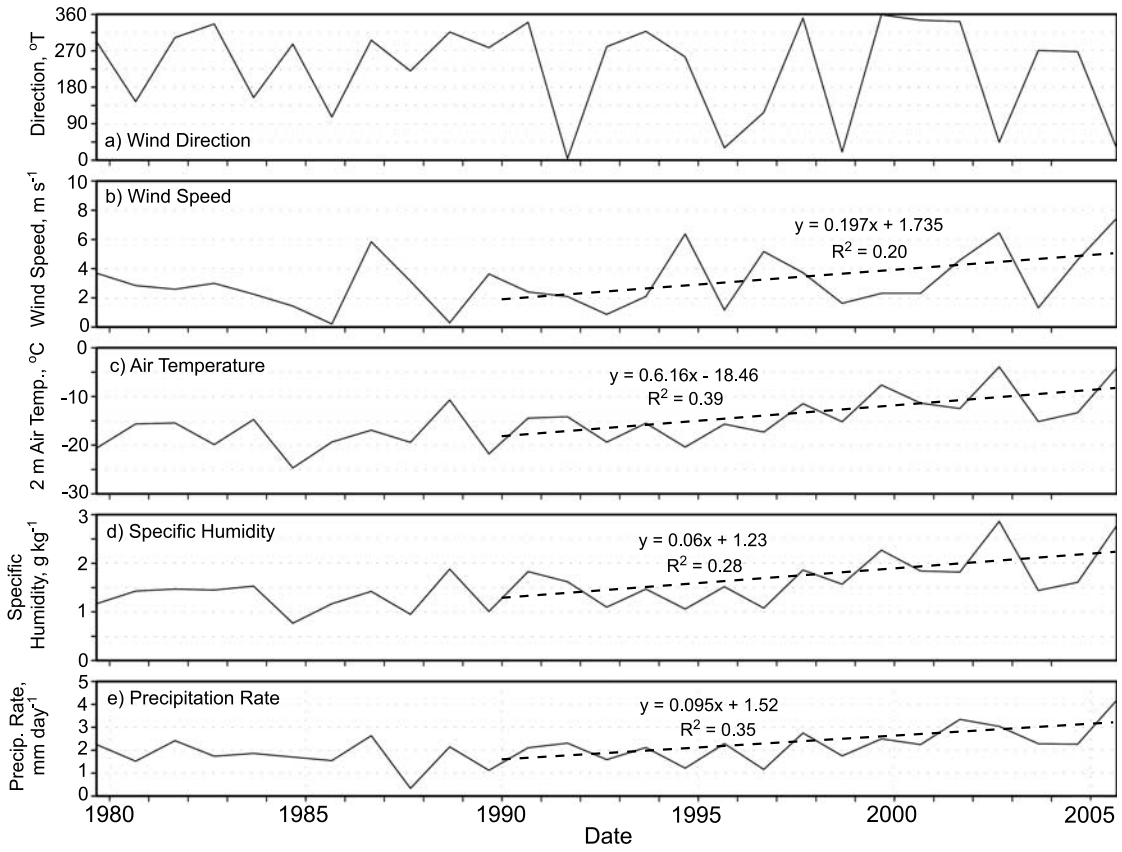

Figure 10. Near-surface monthly mean meteorological (NNR2) data for September from approximately 69.5°S, 90°W for the period 1979–2005: (a) wind direction, (b) wind speed, (c) air temperature, (d) specific humidity, and (e) precipitation rate. Linear regressions are marked from 1990 to 2006.

major impact on ice/snow microstructure and properties as well as on upper ocean structure, i.e., major freshening and stratification relatively early in the season, as was again the case in 2001/2002 [*Massom et al.*, 2006].

[31] A map of modeled ice concentration anomaly data for the late October to early November period of 2005 is shown in Figure 13b, compared to a contemporary AMSR-E concentration image from 8 November (Figure 13a). The strong concentration increase along the WAP coast for this and the November through December period (not shown) is in line with observations in Figures 2 and 7; that is, it strongly reflects wind-driven ice compaction. The impact on modeled regional ice (thermodynamic) production rates is shown in Figure 13c. In general, sea ice production under freezing conditions typically occurs more rapidly in regions of open water than on the base of existing slabs of ice [*Maykut*, 1986]. Figure 13c shows an increased melting of the sea ice at the ice edge in the Eastern Amundsen Sea. This negative ice production is probably due to the northerly wind anomaly (Figures 2, 3, and 14b) advecting warmer air onto the ice and thus melting it. The compensatory role of snow ice formation is unknown, but may be significant given the occurrence of warmer conditions accompanied by relatively heavy snowfall and ice deformation, as was the case in the early spring of 2001/2002 [*Massom et al.*, 2006]. The former is apparent in the modeled snow thickness anomaly map (Figure 13f) and the precipitation rate anomaly map (Figure 12b). Snow ice formation is associated with enhanced snow loading and ice porosity when ice temperatures exceed ~−5°C [*Golden et al.*, 1998], combined with localized dynamic deflection of the ice surface below sea level during deformation [*Massom et al.*, 2001].

[32] Unfortunately, no contemporary in situ observations are available to directly investigate the impact of prolonged dynamic compaction on the regional sea ice thickness distribution. However, model results for late October to early November suggest that the anomalous atmospheric flow led to thicknesses of >5 m (mean) along the western flank of the Antarctic Peninsula (Figure 13d). The associated anomaly map (Figure 13e) shows a thickness anomaly of up to >1 m compared to the long-term late October to early November mean, and a major negative anomaly seaward (due to the ice compaction in 2005). In both cases, the patterns bear a striking resemblance to the actual (satellite-derived) ice edge configuration and concentration (Figure 13a), lending confidence to the model results. This behavior also replicates that during the similar 2001/2002 event, when in situ measurements did confirm an extreme dynamic thickening of the WAP sea ice cover [*Massom et al.*, 2006], in that case to as great as 20 m. For comparison, the usually divergent conditions in the Antarctic sea ice zone overall result in a seasonal cover that is more typically of the order of ~0.5 to 2 m in mean thickness [*Worby et al.*, 1998].

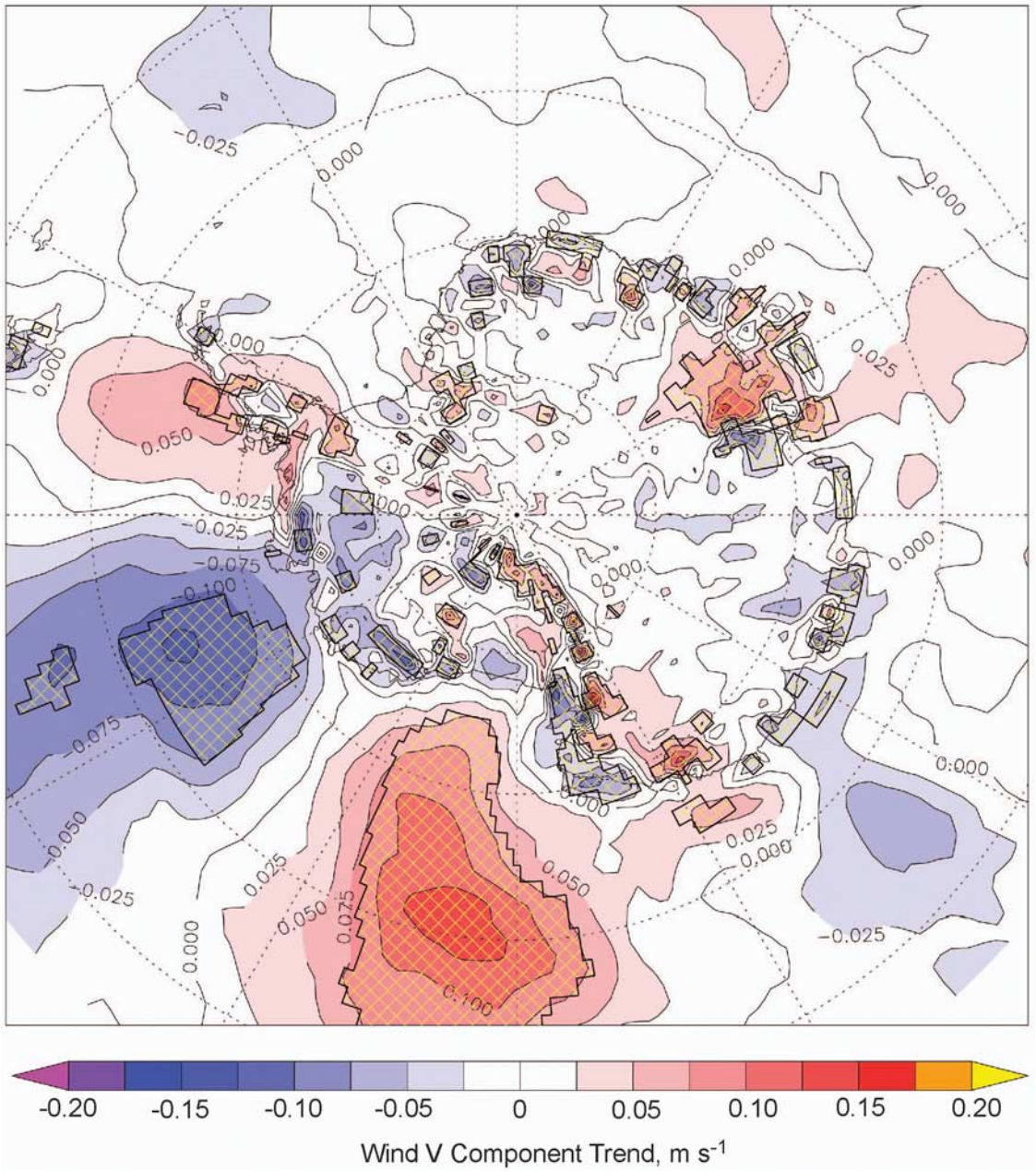

Figure 11. Map of the trend in the September 10 m meridional (V) component of the wind (m s^{-1} per annum) in the combined ECMWF re-analysis (ERA-40) and operational analysis record, 1979–2005. Hatched areas are those with trends statistically significant at less than the 5% level (see text.). Negative trends indicate an increased northerly wind.

[33] Another important impact is that highly compact ice persisted in December 2005 through February 2006 in a sector that typically experiences melt back/retreat of ice to the coast in summer (Figures 2d–2f and 5f). These results are in line with those of *Massom et al.* [2006], who implicated extreme ice compaction and thickness (observed to >20 m) together with an enhanced snow cover thickness in the unusual persistence of the WAP ice cover through the austral summer of 2001/2002. Divergent, low concentration covers tend to melt back more rapidly in summer. Similar findings have also recently emerged from the Ross Sea [*Harangozo and Connolley*, 2006].

4.2. Relative Importance of Short-Term Versus Sustained Wind Events

[34] Having established the importance of wind-forcing, a key question relates to the possible role of strong wind events on submonthly timescales in driving major sea ice retreat and compaction events such as that observed in the late winter-spring of 2005. Figures 5 and 8 indicate that sustained periods of winds with a more dominant northerly

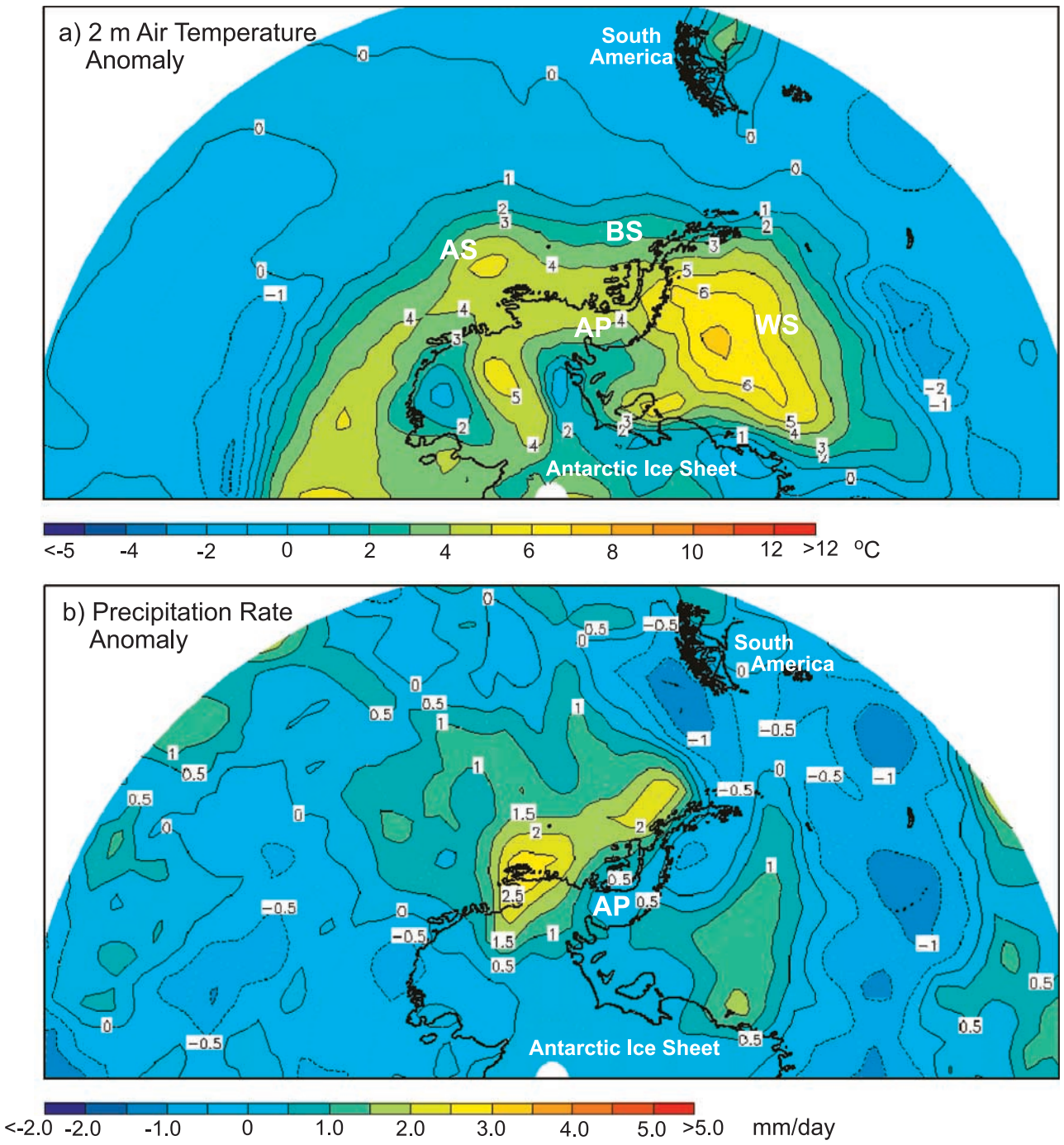

Figure 12. Anomaly maps of (a) near-surface (2 m) air temperature and (b) precipitation rate for October 2005 with respect to the period 1979–2005. AP, Antarctic Peninsula; WS, Weddell Sea; AS, Amundsen Sea; BS, Bellingshausen Sea.

component occurred between about 21 August and 12 September and again between 10 and 23 October 2005. Here we examine 6-hourly to weekly mean MSLP and 10-m wind velocity charts derived from NNR2 data to determine whether one very large meteorological event can create such a linear and compact ice edge and pack or, alternatively, whether it results from a sustained windy period (of weeks). A key question relates to what happened after 23 October; that is, were northerly winds sustained once more, or had the compaction "solidified" the pack in place against the western coast of the Peninsula such that it remained largely intact and persisted, as the leveling out of the time series of ice extent in Figure 8a indicates?

[35] Leading up to, and during, the initial formation of the strong ice edge signature in late August to early September, the weather was dominated (in 6-hourly data) by a series of low-pressure systems developing to the west of the area and tracking southeastward across the coast and inland just to the west of the ice edge feature. This had the effect of maintaining the mean atmospheric flow observed in both

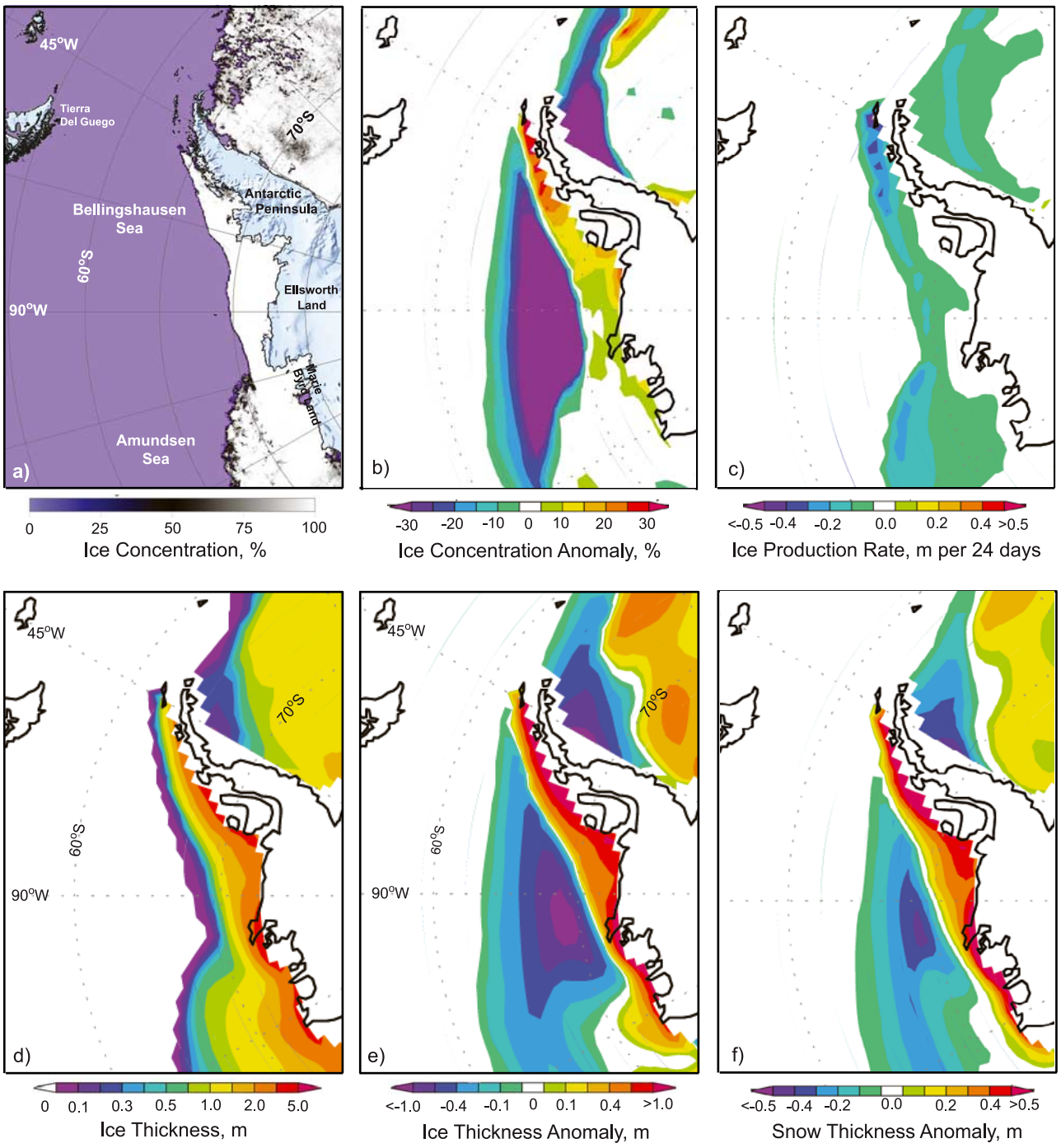

Figure 13. Maps of the WAP region showing (a) AMSR-E derived sea ice concentration map from 8 November 2005, (b) modeled ice concentration anomaly, (c) modeled sea ice production rate, (d) modeled sea ice thickness, (e) modeled ice thickness anomaly, and (f) modeled snow cover thickness anomaly (all for 18 October to 12 November 2005). Further information about the effect of using daily varying precipitation values is given by *Timmermann et al.* [2005].

the monthly and weekly charts (see Figure 14a). From about 13 October 2005, a ridge of high pressure developed just to the west of the Antarctic Peninsula. This coupled with cyclonic activity a west to produce a north to northeasterly flow over the sea ice zone under investigation (Figure 14b). The ridge essentially blocked cyclonic progression with low-pressure systems tracking coastward near 90°W to 100°W. The flow pattern maintained a strong north to northeasterly direction over an extended fetch from north of 60°S to well inland over the west Antarctic plateau.

[36] Prior to the week commencing 14 November, there had been 5 weeks of strong northerly or west-northwesterly flow to set up the observed ice feature. Subsequent events are more complex, with transitory features tracking through

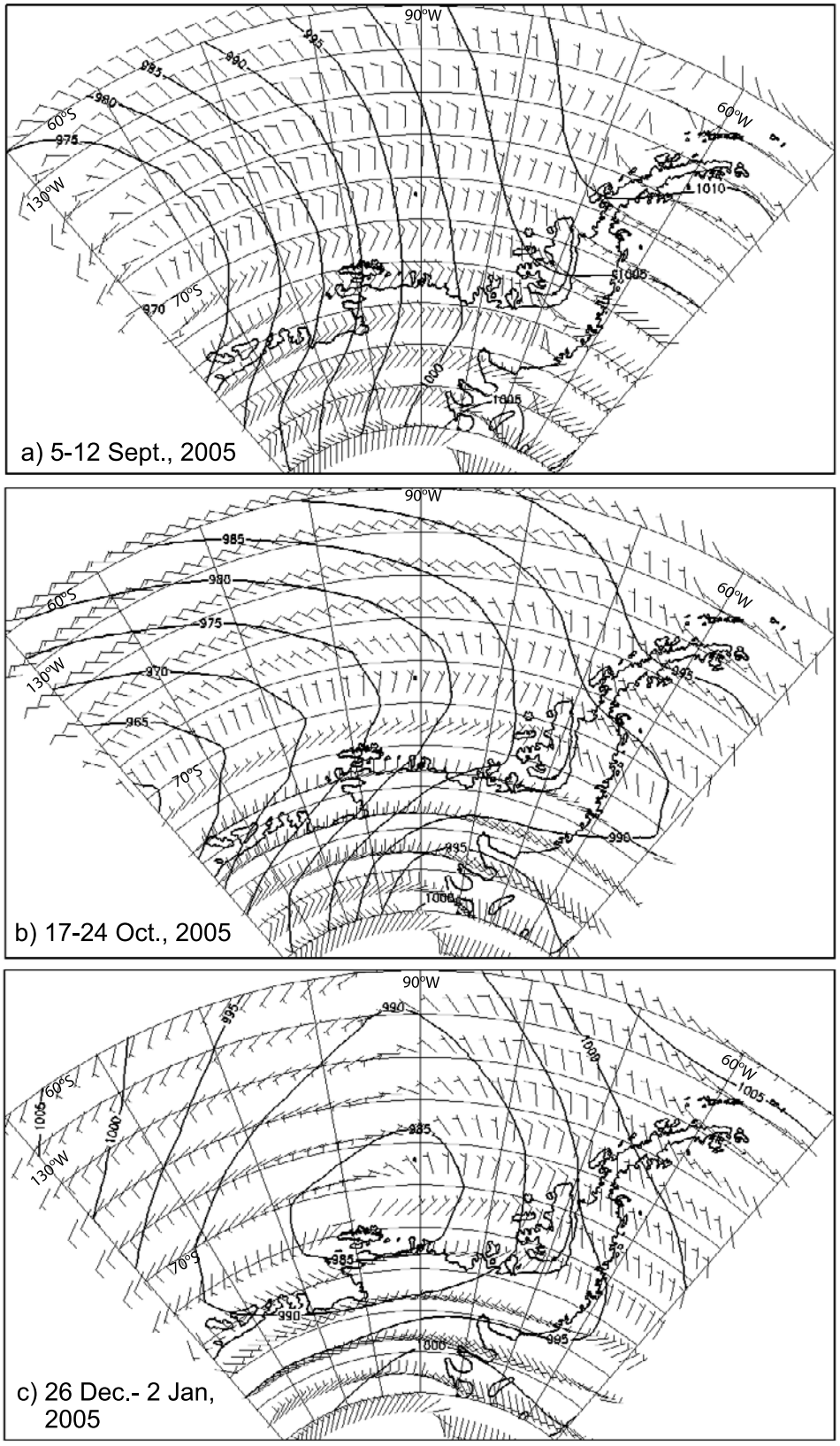

Figure 14. Weekly mean synoptic charts showing mean sea level pressure and 10-m winds (m s^{-1}) for the Antarctic Peninsula region derived from NNR2 data and for the weeks starting on (a) 5 September, (b) 17 October, and (c) 26 December 2005, all at 0000 UT.

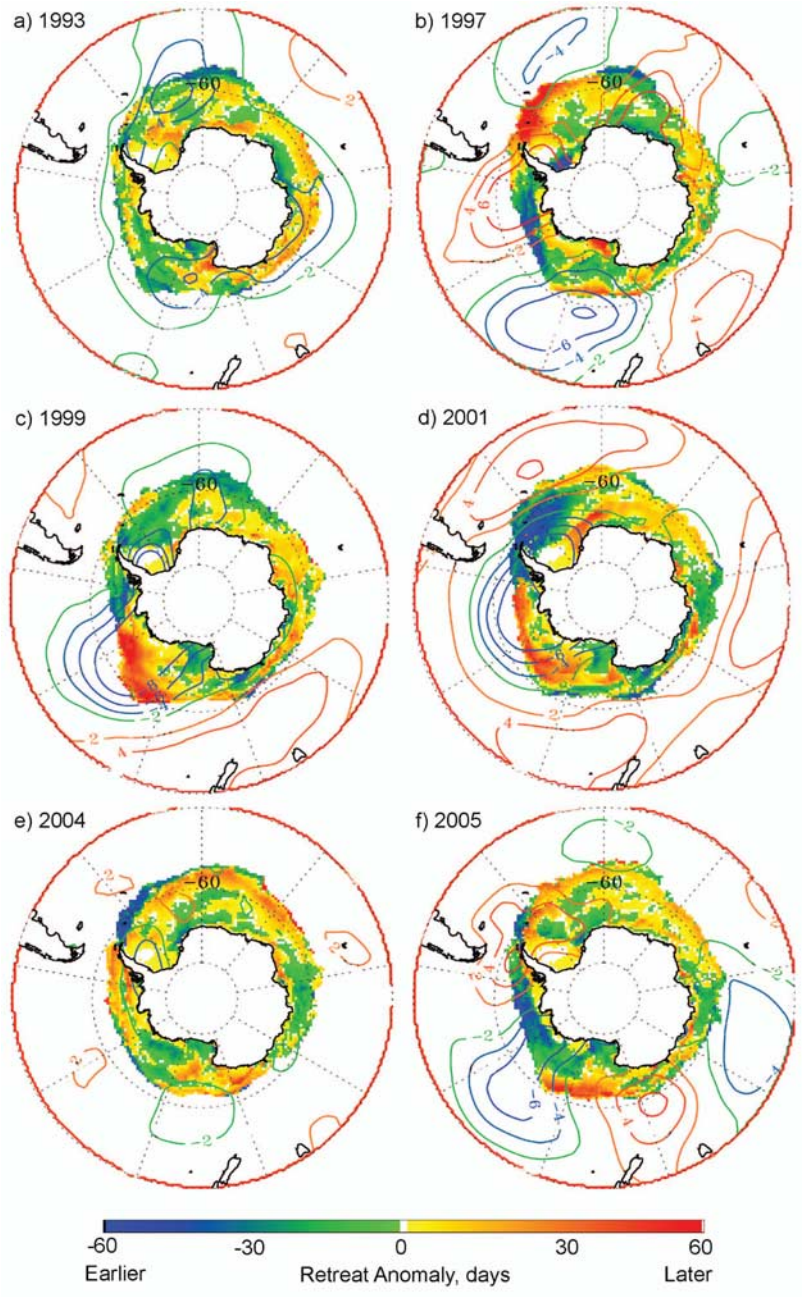

Figure 15. Maps of anomalies in the timing of sea ice retreat in 2005 (derived from SSM/I data) against 1979–2005, along with the anomalies in September-October-November MSLP for (a) 1993, (b) 1997, (c) 1999, (d) 2001, (e) 2004, and (f) 2005. The anomaly has only been calculated where there was sea ice for the month/year in question, and the ice edge contour (15% concentration threshold) is shown.

the area. This is highlighted by a period of easterlies seen on the weekly chart commencing 14 November, and light southwesterlies for the week commencing 21 November (both not shown). The ice edge zone responded by becoming more diffuse after 21 November, but remained considerably more compact than the remaining circum-Antarctic ice edge.

[37] December 2005 was characterized by a more usual pattern of low-pressure systems moving into the WAP and decaying in the Bellingshausen Sea. The first three weeks of the month saw typical south to southeasterly outflows over the sea ice region of interest. However, a low-pressure system became quasi-stationary around 90°W in the last week of the month (starting around 25 December; see Figure 14c) before tracking southward to the east then retrogressing westward along the coast. Subsequent low-pressure systems followed a similar track, maintaining a fresh to strong northwest to northeasterly airflow across the sea ice zone in question. January 2006 did not appear to be particularly anomalous in weather behavior, with lows

Table 1. September-October-November Seasonal Mean of the Standardized Monthly Anomaly for SOI and SAM for the Years Shown in Figure 15[a]

Year	SOI	SAM	Comments
1993	−0.6	+0.6	El Niño and +SAM, mutually neutralizing, weak to no influence (El Niño started dying in July/August)
1997	−1.4	−0.7	El Niño and −SAM, El Niño dominates (super El Niño lasted through June 1998)
1999	+0.9	+0.9	La Niña and +SAM, strongly reinforcing (super La Niña lasted through to about March 2000)
2001	+0.4	+0.9	La Niña (weak) and +SAM, SAM influence dominates
2004	−0.3	−0.01	El Niño (weak) and neutral SAM, weak to no influence
2005	+0.7	+0.2	La Niña and +SAM (weak), La Niña influence dominates

[a]Years 1993, 1997, 1999, 2001, 2004, and 2005.

moving into the WAP region and decaying in the Bellingshausen Sea. The sequence described above suggests that even though northerly wind "events" relaxed as the 2005/2006 summer progressed, the sea ice had been packed in sufficiently against the peninsula that a compact cover persisted; that is, earlier wind events created a heavy ice cover that remained intact as the leveling out of the time series in Figure 8a indicates.

[38] Comparison of NNR2 mean weekly MSLP and 10-m wind velocity charts for late August through late December 2005 with AMSR-E derived daily snapshots of ice extent and concentration (see Figure 5) and the appearance of compact, linear ice edges showed the following temporal sequence:

[39] 1. There were 2 weeks of strong northerly winds, i.e., weeks starting 29 August and 5 September (Figure 14a), with a rapid ice edge recession (see Figure 8a) and the initial appearance of a compact ice edge and pack from ∼80°W to 115°W in early September. Maximum compaction initially occurred on approximately 12 September (see Figures 5b and 8a).

[40] 2. There were 3 of 4 weeks of relatively mild/variable winds, i.e., weeks starting 12 September, 19 September and 3 October (versus 26 September, strong winds), creating two minor ice extent "recoveries" (Figure 8a) and a diffuse ice edge (see Figure 5c, 10 October).

[41] 3. There was 1 week of strong northerly winds, starting 17 October (Figure 14b), leading to another major southward migration of the ice edge and the recreation of a compact ice edge from ∼60°W to 105°W (Figure 5d, 23 October).

[42] 4. There were 2 of 4 weeks of relatively mild or variable winds, i.e., weeks starting 31 October and 14 November (versus strong winds in the weeks starting 24 October and 7 November), with the compact ice edge remaining intact from ∼60°W to 105°W and apparently "solidified in place" (see Figure 5e, 20 November).

[43] 5. Finally, there were 5 weeks of relatively mild or variable winds, weeks starting 21 November through 19 December (see Figure 14c), with the compact ice edge remaining intact (Figure 5f, 26 December).

[44] The above strongly supports the hypothesis that once a compact ice edge was created, it only took one additional week of strong winds to ensure that the compact pack "solidified in place" and thus was largely undisturbed by variable winds thereafter. The atmospheric ridging, discussed above and indicated in Figures 14a (week starting 5 September) and 14b (17 October), appears to be the critical factor in creating the northerly flow over the area under investigation at this time [see also *Harangozo*, 2004a].

4.3. Comparison With Other Years and Events

[45] Interannual variability is further examined by constructing maps of anomalies (with respect to 1979–2005 means) (1) in seasonally averaged SON MSLP and (2) in the timing of the spring sea ice retreat (based on SSM/I ice concentration data). The latter on average begins around September and continues into February (i.e., the mean annual minimum). It should be noted that here we show only the SON MSLP anomalies which coincides with the period over which most of the pack ice is retreating.

[46] Only 4 years out of 26 show strong anomalies toward a sustained early retreat in the South Pacific-WAP sector, namely 1997, 1999, 2001 and 2005. These are compared in Figure 15. Although these anomalies have different spatial locations and extents, all are consistent with the patterns of atmospheric circulation and the location of the major ridge/trough features. Also included are the years 1993 (an event described by *Turner et al.* [2003]) and 2004 (an example of a more typical year).

[47] Table 1 lists the seasonal (i.e., SON) average of the SOI and SAM values for each spring shown in Figure 15. Both have been standardized with respect to 1980–2005, i.e., monthly anomaly divided by the standard deviation for 1980–2005. The following conclusions can be drawn.

[48] 1. Years 1993 and 2004 were near-neutral SOI/SAM springs, consistent with less well organized and weaker overall MSLP anomalies.

[49] 2. Years 1999 and 2001 were strong positive SAM springs, consistent with well-organized, somewhat asymmetrical zonal MSLP anomalies, as described by *Lefebvre et al.* [2004].

[50] 3. Years 1997 and 2005 were strong to moderate SOI signal springs that dominate over moderate to weak SAMs, respectively, consistent with the stronger wave three appearance (which does not occur during strong SAM events), where the austral spring of 1997 was a strong El Niño and that of 2005 was a weak La Niña. This is consistent with the rotation of the zonal wave three structure with respect to 1997 and 2005.

[51] The comments in Table 1 on how ENSO and SAM are thought to mutually interact are based on recent work, i.e., the mutual reinforcement of La Niña/+SAM versus El Niño/-SAM as suggested by *Liu et al.* [2004], *Simmonds and King* [2004], *Carvalho et al.* [2005], *Fogt and Bromwich* [2006], *L'Heureux and Thompson* [2006] and *Stammerjohn et al.* [2008]. We now provide a more detailed comparison of

the ice-atmosphere interactions during the WAP spring retreat of 2005 with other relevant findings described by *Turner et al.* [2003] for 1993, and by *Massom et al.* [2006] for 2001.

4.3.1. Comparison With 1993

[52] As noted above, this year was characterized by a weak El Niño and a positive SAM Index, with the two largely counteracting each other. *Turner et al.* [2003] noted an ice edge retreat of >400 km near 80°W from about 1–15 August in 1993. They attributed this primarily to ice melt brought on by the enhanced temperatures within a strong meridional airflow associated with pronounced high-/low-pressure anomalies on either side of the Antarctic Peninsula, further suggesting that ice dynamics (divergence and compaction) played a secondary role. Events and conditions in 2005 differ in a number of important respects. The retreat in 1993 primarily occurred in the Bellingshausen Sea to the east of 90°W, and there was a large ice extent "recovery" (subsequent northward readvance) in late August/early September 1993. While a major poleward ice edge retreat initially occurred over a 3-week period from mid-August through early September in 2005, conditions in September through November and beyond prevented any such recovery (see section 4.2). The SON MSLP anomalies do not reveal any persistent MSLP features in 1993, consistent with the interpretation that the retreat and subsequent advance/recovery were more of an ephemeral event (compared to 2001 and 2005, for example).

[53] The negative retreat anomaly in the outer pack along 80°W (green patch in Figure 15a) is an area that on average retreats around 7–17 October. In 1993, however, retreat occurred 38 days earlier in the location of the outer edge of this anomaly (on 30 August instead of 7 October) and ~16 days earlier just inside this location (in mid to late September instead of early to mid October). Although the >400-km retreat that *Turner et al.* [2003] observed on 1–15 August is not revealed here (because we track the last, or final, retreat for that year), the new results show that this area did, in spite of the recovery, experience an anomalously early retreat (perhaps because of the preconditioning caused by the earlier episodic retreat).

4.3.2. Comparison With 2001

[54] In some ways, the unusual atmospheric circulation in the 2005 spring resembled that in the 2001 spring-summer. A marked zonal wave three pattern [*Raphael*, 2004, 2007] prevailed in both cases (Figure 3 and Figure 3 of *Massom et al.* [2006]), giving rise to negative 500-hPa height anomalies in the South Pacific and positive anomalies in the low- to mid-latitude South Atlantic. This resulted in persistence of dominant northerly winds across the WAP. There were, however, two crucial differences in the average circulation in October–November 2005: (1) the Pacific trough, at 130°W, was ~40° west of that in October 2001 to February 2002 (although the Pacific trough in October 2001 (not shown) was at a similar location), and (2) the positive 500-hPa height anomaly in the South Atlantic extended south over the Weddell and eastern Bellingshausen seas. As a result, the east-west pressure gradient in the South Pacific was enhanced in 2005, resulting in winds with a stronger northerly component affecting most of the South Pacific over most of the spring (unlike 2001). This is consistent with the westward extension of compacted ice and marked negative sea ice concentration anomalies in the spring of 2005 compared to 2001.

[55] Reasons for these similarities and differences are not clear. As has been noted, the Southern Annular Mode (SAM) was weak in late 2005. During strong SAM phases, negative ice extent anomalies are confined to the WAP area in late winter and early spring [*Lefebvre et al.*, 2004], but this was clearly not the case in 2005. To some extent, the dipole pattern of opposing sea ice concentration anomalies in the Bellingshausen and Weddell seas, that is most clear in October 2005 (Figure 7c), resembles the Antarctic Dipole pattern expected for La Niña events [*Yuan and Martinson*, 2001]. Between August and October 2005, the SOI reversed sign from negative to positive with values of −1.3 to +1.9, and remained weakly negative into the southern summer.

[56] The WAP sea ice anomaly in August–November 2005 resembles that in September 2001 to February 2002, i.e., rapid ice retreat accompanied by extreme compaction with associated enhanced temperatures and snowfall. In 2001, an ice edge retreat of ~300 km took place at 70°W from 28 September to 16 October [*Massom et al.*, 2006], compared to a similar total retreat of 315 km centered on ~90°W over a 3-week period (i.e., 29 August to 9 September and 17–23 October) in 2005. In both 2001 and 2005, the ice retreat was primarily due to dynamic ice compaction (convergence) associated with strong and persistent meridional atmospheric flow, although ice melt and a change in ice production likely also played a role. This resulted in a highly compact marginal ice zone (linear ice edge) and ice cover in general. Moreover, maximum ice extent occurred significantly earlier than the norm in both years, i.e., in mid-August in 2005 and July in 2001 [*Massom et al.*, 2006] compared to late September in 2004. Spring 2004 serves as a distinct contrast to 2005, with its neutral ENSO and SAM indices and weak MSLP anomalies, contributing to near zero to weakly positive sea ice retreat anomalies.

[57] In 2001, major negative ice extent anomalies occurred not only in the WAP [*Massom et al.*, 2006] but also in the western Weddell Sea [*Turner et al.*, 2002]. This led to an earlier ice edge retreat, as shown in Figure 15d and consistent with the negative regional trend in ice season duration reported by *Parkinson* [2004]. The "extremeness" of this year is revealed by the large and persistent low MSLP anomaly centered roughly on 90°W but extending across and into the East Antarctic Peninsula, together with a highly anomalous early sea ice retreat just west of the peninsula and throughout the western Weddell outer pack ice region, all in the vicinity of the eastern limb of the MSLP anomaly. This is in contrast to the anomalously late sea ice retreats farther to the west in the vicinity of the western limb of the MSLP anomaly. A thin line of positive (late) retreat anomalies is present right up against the WAP, i.e., the area of compacted thick sea ice that persisted well into late summer, as described by *Massom et al.* [2006].

[58] The weakly positive SOI and the development of negative tropical sea-surface temperature anomalies (not shown) in the 2005 spring indicate the onset of weak La Niña conditions. Again, however, the below-normal sea ice concentrations/extent in the Amundsen Sea at this time (Figure 7) are unusual because *Yuan and Martinson* [2001] showed that sea ice is, on average, more extensive here during La Niña events in austral winter and spring.

This reflects the fact that such events are usually driven by southerly winds in this region associated with a trough centered around 100°W, i.e., much farther east than the 2005 spring. Moreover, the widespread negative ice anomalies in 2001 spring in the South Pacific and Weddell Sea did not resemble the Antarctic Dipole pattern [*Massom et al.*, 2006] and the SOI again was, in general, only slightly positive. These coincided with a weak La Niña and positive SAM, which had a tendency to reinforce each other to lead to a deepening of the Amundsen-Bellingshausen Low.

[59] Some of the differences in the extratropical atmospheric circulation between 2005 and 2001 will simply be because of its internal variability. However, the South Pacific circulation anomalies in the Septembers of both 2005 and 2001 clearly project onto a trend in the September 10-m meridional wind field over 1979–2005 (Figure 11), at least in the area west of the WAP. In particular, and as noted earlier, there is a statistically significant increase of the northerly wind component between 110 and 125°W (Figure 11), and an equally marked opposite change over and north of the Ross Sea in this month. In the winter sea ice zone at 69°S, 100°W, the monthly average meridional wind components in the Septembers of 2005 (-6.2 m s^{-1}) and 2001 (-4.1 m s^{-1}) were the strongest and third strongest, respectively, in the entire ERA-40/ECMWF operational record. The zonal wave three patterns [see *Raphael*, 2004, 2007] in the 2005 and 2001 spring average circulation are not, however, mirrored in the trends in the combined ECMWF reanalyzed and analyzed meridional wind record. No clear trends occur in other spring months.

5. Conclusions

[60] In September–October 2005, the juxtaposition of quasi-stationary low and high mean sea level pressure anomalies at 130°W and 60°W, respectively, created strong and persistent northerly and strong airflow across the West Antarctic Peninsula. This pattern, which was part of a hemispheric zonal wave three configuration, had a major impact on sea ice and weather conditions in a region that has experienced considerable recent change. It led to extreme ice compaction (convergence) in the Bellingshausen and East Amundsen seas (60°W–130°W) but divergence in the West Amundsen and East Ross seas. Model results suggest that the former caused major dynamic sea ice thickening along the entire WAP region, as also observed by *Massom et al.* [2006] during a field campaign in 2001/2002. As in 2001/2002, the strong atmospheric circulation anomaly created a major negative ice extent anomaly and an unusually rapid sea ice retreat for the region. As a result, maximum ice extent occurred significantly earlier (in mid-August) than average (September–October). Episodes such as this have a first-order impact on trends in ice season duration [*Stammerjohn et al.*, 2008], and contribute to the overall negative trend in the WAP region (as reported by *Parkinson* [2004]).

[61] These results support the idea that recent negative ice extent anomalies observed in the WAP region in late winter through spring appear to be predominantly dynamically driven, and are in line with those of *Harangozo* [2006], *Massom et al.* [2006] and *Turner et al.* [2002], and the synoptic-scale studies of the region by *Stammerjohn et al.* [2003] and *Harangozo* [2004a]. The physical blocking effect of the Antarctic Peninsula is a key factor, and one that sets this area apart from other Antarctic sectors. Indeed, this is the largest meridional barrier to sea ice drift/advection anywhere around Antarctica, running from ~73°S to 61°S (including islands). As noted by *van den Broeke* [2000], the pronounced south-north orientation of the Peninsula makes it more sensitive to circulation changes with a zonal component than other sectors of the Antarctic coast.

[62] Analysis of the relative role of short-term versus more sustained wind-forcing events in 2005 suggests that once a compact ice edge was created, it only took one additional week of strong winds to ensure that the heavily compacted and dynamically thickened pack "solidified in place" to remain intact and largely undisturbed by variable winds thereafter. With its relatively high moisture content, the more northerly airstream also resulted in higher than average snowfall in the WAP region (precipitation rate anomalies to >2.5 mm/d). As shown in 2001/2002, this can lead to widespread snow ice formation [*Massom et al.*, 2006], which could to some extent counterbalance any ice mass loss by melt associated with the unseasonably high surface air temperatures. A thicker snow cover could also contribute to the observed unusual survival of compact ice in the WAP sector through the summer melt season in both 2005/2006 and 2001/2002, owing to its insulative properties [*Eicken et al.*, 1995].

[63] A somewhat surprising result is the strength of apparently positive trends in NNR2-derived wind speed, air temperature, specific humidity and precipitation rate at a point in the Bellingshausen Sea (~69.5°S, 95°W) since about 1990. Further investigation unearthed an apparent discrepancy between the NNR2 record and in situ observations at Rothera, while the ERA-40 record largely replicated the latter. However, the ERA-40 results farther seaward (70.0°S, 90.0°W) displayed the same upward trends in air temperature and specific humidity as the NNR2 record. Clearly, this requires further investigation (preferably using additional independent data), given the extensive use of these data sets in climate-related studies.

[64] The results presented here again suggest that pack ice recession and enhanced temperatures are intimately coupled in the WAP region, in that they are both "driven" by sustained episodes of winds with a dominant northwesterly component. A statistically significant increase in the northerly 10-m wind component between 110°W and 125°W in the Septembers of 1979–2005, and an equally marked opposite change over and north of the Ross Sea in this month, is noted. No clear trends occur in other spring months. In the late winter-spring of 2005 and the late winter through summer of 2001/2002 [*Massom et al.*, 2006], the configuration of low- and high-pressure anomalies transported relatively warm air over a region that has been undergoing a significant warming trend over the past half century [*Smith et al.*, 1999; *Vaughan et al.*, 2003], and likely contributed to that trend; that is, it led to surface air temperature anomalies of +1°C to +5°C. These results support those of *King and Harangozo* [1998] in suggesting that this warming is associated with an increase in the northerly component of the atmospheric

circulation over the Peninsula. Indeed, the 2005/2006 summer was among the warmest over the past 30 years on the basis of data from six weather stations in the region [*Skvarca et al.*, 2006].

[65] The possible ramifications of the observed changes in sea ice distribution and characteristics are complex and poorly understood. If the sea ice zone is now more regularly compacted and pushed back toward the coast, it follows that less ice reaches low latitudes, leading to less melting and freshwater input there. This could contribute to the increasing salinity of the upper ocean in the region in summer [*Meredith and King*, 2005]. *Nihashi and Ohshima* [2001] speculate that interannual variability in sea ice extent (and concentration and thickness) can impact annual heat storage in the ocean, and as such will affect subsequent patterns of ice advance and retreat [see also *Comiso and Gordon*, 1998]. Ice edge location is also of major ecological significance, with the marginal ice zone and adjacent ocean being regions of concentrated biological activity at all trophic levels [*Ainley and Jacobs*, 1981; *Fraser and Ainley*, 1986; *Ribic et al.*, 1991; *Smith and Nelson*, 1986]. The reduced ice extent is itself likely to impact surface temperature through poorly understood feedback mechanisms [*Stammerjohn and Smith*, 1996; *van den Broeke*, 2000; *Stammerjohn et al.*, 2008]; that is, more of the low-albedo open ocean is exposed to the atmosphere at an earlier date, with major implications for the surface heat, momentum and radiation budgets. Following *Menendez et al.* [1999] and *Murray and Simmonds* [1995], the unusual sea ice distribution in 2005 may also result in changes in cyclone trajectories.

[66] Given that the structure and function of all levels of the Antarctic marine ecosystem are intimately coupled to the annual advance, retreat, behavior and characteristics of the sea ice cover [*Smith et al.*, 1995; *Ainley et al.*, 2003], extreme changes such as those described here are likely to have a significant impact on regional ecology. Indeed, conditions in late 2005 perpetuate the recent shortening of the regional sea ice duration, and contribute to the apparent gradual replacement of the continental, polar régime characteristic of the southern WAP with a more maritime and warmer régime [*Smith et al.*, 2003]. By the same token, such conditions may contribute to observed sensitive ecosystem responses to sea ice changes that are becoming increasingly apparent [*Chapman et al.*, 2004; *Fraser and Hofmann*, 2003; *Smith et al.*, 1999, 2003]. Moreover, associated above-average snowfalls can negatively impact the breeding success of Adélie penguin (*Pygoscelis adeliae*) populations in the WAP region [*Fraser et al.*, 1992; *Massom et al.*, 2006].

[67] Variability such as that observed in 2005 has wide-ranging implications, given the key role that sea ice plays in the global climate system by influencing the regional heat budget, surface albedo, and consequently oceanic and atmospheric circulation. Highly complex mechanisms and feedbacks clearly result, underlining the critical need for further research. As stressed by *Turner et al.* [2003], a major challenge is to accurately represent the development of major sea ice anomalies such as those described here in global models designed to simulate the present and predict future climate-change scenarios.

[68] **Acknowledgments.** For R. M., this work was supported by the Australian Government's Cooperative Research Centres Programme through the Antarctic Climate and Ecosystems Cooperative Research Centre (ACE CRC). NCEP/NCAR Re-analysis 2 data were acquired from NOAA via http://www.cdc.noaa.gov/cdc/reanalysis/reanalysis.shtml. ERA-40 data were obtained from the European Centre for Medium-Range Weather Forecasting Reanalysis project, and were supplied to the British Antarctic Survey by the British Atmospheric Data Centre. This study is supported for W.L. by the Federal Science Office (Belgium). For C.F., this work was supported by NASA grant NNG04GP50G. Meteorological data from Rothera Station were obtained from the British Antarctic Survey at: http://www.antarctica.ac.uk/cgi-bin/metdb-form-2.pl?tabletouse=U_MET.ROTHERA_SYNOP&complex=1&idmask=. . .&acct=cmet. SAM index data were obtained from Gareth Marshall (BAS) at: http://www.nerc-bas.ac.uk/icd/gjma/sam.html. SSM/I ice-concentration data were obtained from the NASA Earth Observing System Distributed Active Archive Center (DAAC) at the U.S. National Snow and Ice Data Center, University of Colorado, Boulder (http://www.nsidc.org). MODIS data were obtained from NASA's Distributed Active Archive Center. Thanks are extended to Ben Raymond (Australian Antarctic Division) for help with the ice motion data. The helpful suggestions provided by two anonymous reviewers and Stan Jacobs (Lamont Doherty Earth Observatory, USA), Phil Reid (Australian BoM and ACE, CRC), and Jan Lieser (ACE CRC) are much appreciated.

References

Ainley, D. G., and S. S. Jacobs (1981), Seabird affinities for ocean and ice boundaries in the Antarctic, *Deep Sea Res., Part A*, *28*, 1173–1185.

Ainley, D. G., C. T. Tynan, and I. Stirling (2003), Sea ice: A critical habitat for polar marine mammals and birds, in *Sea Ice—An Introduction to its Physics, Biology, Chemistry and Geology*, edited by D. Thomas and G. Dieckmann, pp. 240–266, Blackwell Sci., Oxford, U. K.

Brierley, A. S., and D. N. Thomas (2002), Ecology of Southern Ocean pack ice, *Adv. Mar. Ecol.*, *43*, 171–276.

Carvalho, L. M. V., C. Jones, and T. Ambrizzi (2005), Opposite phases of the Antarctic Oscillation and relationships with intraseasonal to interannual activity in the Tropics during austral summer, *J. Clim.*, *18*, 702–718.

Chapman, E. W., C. A. Ribic, and W. R. Fraser (2004), The distribution of seabirds and pinnepeds in Marguerite Bay and their relationship to physical features during austral winter 2001, *Deep Sea Res., Part II*, *51*, 2261–2278.

Comiso, J. C. (1995), SSM/I concentrations using the Bootstrap algorithm, *NASA Ref. Publ., 1380*, 40 pp.

Comiso, J. C. (2003), Large-scale characteristics and variability of the global sea ice cover, in *Sea Ice—An Introduction to its Physics, Biology, Chemistry and Geology*, edited by D. Thomas and G. Dieckmann, pp. 112–142, Blackwell Sci., Oxford, U. K.

Comiso, J. (2005), Bootstrap sea ice concentrations for Nimbus-7 SMMR and DMSP SSM/I, June to September 2001, updated 2005, http://nsidc.org/data/nsidc-0079.html, Natl. Snow and Ice Data Cent., Boulder, Colo.

Comiso, J. C., and A. L. Gordon (1998), Interannual variability in summer sea ice minimum, coastal polynyas and bottom water formation in the Weddell Sea, in *Antarctic Sea Ice: Physical Processes, Interactions and Variability*, *Antarct. Res. Ser.*, vol. 74, edited by M. Jeffries, pp. 293–315, AGU, Washington D. C.

Eicken, H., H. Fischer, and P. Lemke (1995), Effects of the snow cover on Antarctic sea ice and potential modulation of its response to climate change, *Ann. Glaciol.*, *21*, 369–376.

Emery, W. J., C. W. Fowler, and J. A. Maslanik (1995), Satellite remote sensing of ice motion, in *Oceanographic Applications of Remote Sensing*, edited by M. Ikeda and F. W. Dobson, pp. 367–379, CRC Press, Boca Raton, Fla.

Fichefet, T., and M. Morales-Maqueda (1997), Sensitivity of a global sea ice model to the treatment of ice thermodynamics and dynamics, *J. Geophys. Res.*, *102*, 12,609–12,646.

Fogt, R. L., and D. H. Bromwich (2006), Decadal variability of the ENSO teleconnection to the high latitude South Pacific governed by coupling with the Southern Annular Mode, *J. Clim.*, *19*, 979–997.

Fowler, C. (2003), *Polar Pathfinder Daily 25 km EASE-Grid Sea Ice Motion Vectors*, http://nsidc.org/data/nsidc-0116.html, Natl. Snow and Ice Data Cent., Boulder, Colo.

Fraser, W. R., and D. G. Ainley (1986), Ice edges and seabird occurrence in Antarctica, *BioScience*, *36*(4), 258–263.

Fraser, W. R., and E. E. Hofmann (2003), A predator's perspective on causal links between climate change, physical forcing and ecosystem response, *Mar. Ecol. Prog. Ser.*, *265*, 1–15.

Fraser, W. R., W. Z. Trivelpiece, D. G. Ainley, and S. G. Trivelpiece (1992), Increases in Antarctic penguin populations: Reduced competition with

whales or a loss of sea ice due to environmental warming?, *Polar Biol.*, *11*, 525–531.
Golden, K. M., S. F. Ackley, and V. I. Lytle (1998), The percolation phase transition in sea ice, *Science*, *282*, 2238–2241.
Goosse, H., and T. Fichefet (1999), Importance of ice-ocean interactions for the global ocean circulation: a model study, *J. Geophys. Res.*, *104*, 23,337–23,355.
Hall, A., and M. Visbeck (2002), Synchronous variability in the Southern Hemisphere atmosphere, sea ice, and ocean resulting from the Annular Mode, *J. Clim.*, *15*, 3043–3057.
Harangozo, S. A. (1997), Atmospheric meridional circulation impacts on contrasting winter sea ice extent in two years in the Pacific sector of the Southern Ocean, *Tellus, Ser. A*, *49*, 388–400.
Harangozo, S. A. (2000), A search for ENSO teleconnections in the west Antarctic Peninsula climate in austral winter, *Int. J. Climatol.*, *20*, 663–679.
Harangozo, S. A. (2004a), The impact of winter ice retreat on Antarctic winter sea ice extent and links to atmospheric meridional circulation, *Int. J. Climatol.*, *24*, 1023–1044.
Harangozo, S. A. (2004b), The relationship of Pacific deep tropical convection to the winter and springtime extratropical atmospheric circulation of the South Pacific in El Niño events, *Geophys. Res. Lett.*, *31*, L05206, doi:10.1029/2003GL018667.
Harangozo, S. A. (2006), Atmospheric circulation impacts on winter maximum sea ice extent in the west Antarctic Peninsula region (1979–2001), *Geophys. Res. Lett.*, *33*, L02502, doi:10.1029/2005GL024978.
Harangozo, S. A., and W. M. Connolley (2006), The role of atmospheric circulation in the record minimum extent of open water in the Ross Sea in the 2003 austral summer, *Atmos. Ocean*, *44*(1), 83–97.
Hines, K. M., D. H. Bromwich, and G. J. Marshall (2000), Artificial surface pressure trends in the NCEP/NCAR reanalysis over the Southern Ocean and Antarctica, *J. Clim.*, *12*, 3940–3952.
Intergovernmental Panel on Climate Change (2001), *IPCC Report on Climate Change 2001. The Scientific Basis, Contribution of Working Group 1 to the Third Assessment Report of the Intergovernmental Panel on Climate Change*, 881 pp., Cambridge Univ. Press, New York.
Jacobs, S. S., and J. C. Comiso (1997), Climate variability in the Amundsen and Bellingshausen seas, *J. Clim.*, *10*, 697–709.
Kalnay, E., et al. (1996), The NCEP/NCAR 40-year reanalysis project, *Bull. Am. Meteorol. Soc.*, *77*, 437–471.
Karoly, D. J. (1989), Southern Hemisphere circulation features associated with El Niño–Southern Oscillation events, *J. Clim*, *2*, 1239–1252.
Kern, S. L., and D. A. Clausi (2003), A Comparison of two 85 GHz SSM/I ice concentration algorithms with AVHRR and ERS-SAR, *IEEE Trans. Geosci. Remote Sens.*, *41*(10), 2294–2306.
Kiladis, G. N., and K. C. Mo (1998), Interannual and intraseasonal variability in the Southern Hemisphere, in *Meteorology of the Southern Hemisphere*, edited by D. J. Karoly and D. G. Vincent, *Meteorol. Monogr.*, *27*(49), 307–336.
King, J. C., and S. A. Harangozo (1998), Climate change in the western Antarctic Peninsula since 1945: Observations and possible causes, *Ann. Glaciol.*, *27*, 571–575.
Kwok, R., and J. C. Comiso (2002a), Spatial patterns of variability in Antarctic surface temperature: Connections to the Southern Hemisphere Annular Mode and the Southern Oscillation, *Geophys. Res. Lett.*, *29*(14), 1705, doi:10.1029/2002GL015415.
Kwok, R., and J. C. Comiso (2002b), Southern Ocean climate and sea ice anomalies associated with the Southern Oscillation, *J. Clim.*, *15*, 487–501.
Lachlan-Cope, T., and W. Connolley (2006), Teleconnections between the tropical Pacific and the Amundsen-Bellingshausen Sea: Role of the El Niño/Southern Oscillation, *J. Geophys. Res.*, *111*, D23101, doi:10.1029/2005JD006386.
Lefebvre, W., and H. Goosse (2008), An analysis of the atmospheric processes driving the large-scale winter sea ice variability in the Southern Ocean, *J. Geophys. Res.*, doi:10.1029/2006JC004032, in press.
Lefebvre, W., H. Goosse, R. Timmermann, and T. Fichefet (2004), Influence of the Southern Annular Mode on the sea ice-ocean system, *J. Geophys. Res.*, *109*, C09005, doi:10.1029/2004JC002403.
L'Heureux, M. L., and D. W. J. Thompson (2006), Observed relationships between the El Niño/Southern Oscillation and the extra-tropical zonal-mean circulation, *J. Clim.*, *19*, 276–287.
Liu, J., J. A. Curry, and D. G. Martinson (2004), Interpretation of recent Antarctic sea ice variability, *Geophys. Res. Lett.*, *31*, L02205, doi:10.1029/2003GL018732.
Loeb, V., V. Siegel, O. Holm-Hansen, R. Hewitt, W. Fraser, W. Trivelpiece, and S. Trivelpiece (1997), Effects of sea-ice extent and salp or krill dominance on the Antarctic food web, *Nature*, *387*, 897–900.
Madec, G., P. Delecluse, M. Imbard, and C. Lévy (1999), OPA 8.1 ocean general circulation model reference manual, Notes du Pôle de Model. 11, 91 pp., Inst. Pierre-Simon Laplace, Jussieu, France.
Marshall, G. J. (2003), Trends in the Southern Annular Mode from observations and reanalyses, *J. Clim.*, *16*, 4134–4143.
Marshall, G. J., and S. A. Harangozo (2000), An appraisal of NCEP/NCAR reanalysis MSLP data viability for climate studies in the South Pacific, *Geophys. Res. Lett.*, *27*, 3057–3060.
Massom, R. A., et al. (2001), Snow on Antarctic sea ice, *Rev. Geophys.*, *39*(3), 413–445.
Massom, R. A., et al. (2006), Extreme anomalous atmospheric circulation in the West Antarctic Peninsula region in austral spring and summer 2001/2, and its profound impact on sea ice and biota, *J. Clim.*, *19*, 3544–3571.
Maykut, G. A. (1986), The surface heat and mass balance, in *The Geophysics of Sea Ice*, *NATO ASI Ser. B*, vol. 146, edited by N. Untersteiner, pp. 395–463, Plenum, New York.
Menendez, C. G., V. Serafini, and H. Le Treut (1999), The storm tracks and energy cycle of the Southern Hemisphere: Sensitivity to sea-ice boundary conditions, *Ann. Geophys.*, *17*(11), 1478–1492.
Meredith, M. P., and J. C. King (2005), Rapid climate change in the ocean west of the Antarctic Peninsula during the second half of the 20th century, *Geophys. Res. Lett.*, *32*, L19604, doi:10.1029/2005GL024042.
Murray, R. J., and I. Simmonds (1995), Responses of climate and cyclones to reductions in Arctic winter sea ice, *J. Geophys. Res.*, *100*, 4791–4806.
Nicol, S., T. Pauly, N. L. Bindoff, S. Wright, D. Thiele, G. W. Hosie, P. G. Strutton, and E. Woehler (2000), Ocean circulation off East Antarctica affects ecosystem structure and sea-ice extent, *Nature*, *406*, 504–507.
Nihashi, S., and K. I. Ohshima (2001), Relationship between ice decay and solar heating through open water in the Antarctic sea ice zone, *J. Geophys. Res.*, *106*, 16,767–16,782.
Orsi, A. H., T. Whitworth III, and W. D. Nowlin Jr. (1995), On the meridional extent and fronts of the Antarctic Circumpolar Current, *Deep Sea Res., Part I*, *42*, 641–673.
Parkinson, C. L. (2004), Southern Ocean sea ice and its wider linkages: Insights revealed from models and observations, *Antarct. Sci.*, *16*(4), 387–400.
Raphael, M. N. (2003), Recent, large-scale changes in the extra-tropical Southern Hemisphere atmospheric circulation, *J. Clim.*, *16*, 2915–2924.
Raphael, M. N. (2004), A zonal wave 3 index for the Southern Hemisphere, *Geophys. Res. Lett.*, *31*, L23212, doi:10.1029/2004GL020365.
Raphael, M. N. (2007), The influence of atmospheric zonal wave three on Antarctic sea ice variability, *J. Geophys. Res.*, *112*(D12), D12112, doi:10.1029/2006JD007852.
Renwick, J. A. (2002), Southern Hemisphere circulation and relations with sea ice and sea surface temperature, *J. Clim.*, *15*, 3058–3068.
Ribic, C. A., D. G. Ainley, and W. R. Fraser (1991), Habitat selection by marine mammals in the marginal ice zone, *Antarct. Sci.*, *3*, 181–186.
Simmonds, I., and K. Keay (2000), Variability of Southern Hemisphere extratropical cyclone behaviour 1958–97, *J. Clim.*, *13*, 550–561.
Simmonds, I., and J. C. King (2004), Global and hemispheric climate variations affecting the Southern Ocean, *Antarct. Sci.*, *16*, 401–413.
Skvarca, P., F. Rau, T. Scambos, H. Sala, Y. Yermolin, and J. Thom (2006), Effects of ongoing climatic warming on the cryosphere of the Antarctic Peninsula, paper presented at International Symposium on Cryospheric Indicators of Global Climate Change, Int. Glaciol. Soc., Cambridge, U. K.
Smith, R. C., and S. E. Stammerjohn (2001), Variations of surface air temperature and sea ice extent in the western Antarctic Peninsula (WAP) region, *Ann. Glaciol.*, *33*, 493–500.
Smith, R. C., et al. (1995), The Palmer LTER: A long-term ecological research program at Palmer Station, Antarctica, *Oceanography*, *8*(3), 77–86.
Smith, R. C., et al. (1999), Marine ecosystem sensitivity to climate change, *BioScience*, *49*, 393–404.
Smith, R. C., W. R. Fraser, and S. E. Stammerjohn (2003), Climate variability and ecological response of the marine ecosystem in the Western Antarctic Peninsula (WAP) region, in *Climate Variability and Ecosystem Response at Long-Term Ecological Research (LTER) Sites, D. Greenland*, edited by D. G. Goodin and R. C. Smith, pp. 158–173, Oxford Univ. Press, Oxford, U. K.
Smith, W. O., Jr., and D. M. Nelson (1986), Importance of ice edge phytoplankton production in the Southern Ocean, *BioScience*, *36*, 251–257.
Squire, V. A., P. Wadhams, P. J. Rottier, and A. K. Liu (1995), Of ocean waves and sea ice, *Annu. Rev. Fluid Mech.*, *27*, 115–168.
Stammerjohn, S. E., and R. C. Smith (1996), Spatial and temporal variability in Western Antarctic Peninsula sea ice coverage, in *Foundations for Ecological Research West of the Antarctic Peninsula*, *Antarct. Res. Ser.*, vol. 70, edited by R. M. Ross, E. Hofmann, and L. B. Quetin, pp. 81–104, AGU, Washington D. C.
Stammerjohn, S. E., and R. C. Smith (1997), Opposing Southern Ocean climate patterns as revealed by trends in sea ice coverage, *Clim. Change*, *37*, 617–639.
Stammerjohn, S. E., M. R. Drinkwater, R. C. Smith, and X. Liu (2003), Ice-atmosphere interactions during sea-ice advance and retreat in the western

Antarctic Peninsula region, *J. Geophys. Res.*, *108*(C10), 3329, doi:10.1029/2002JC001543.

Stammerjohn, S. E., D. G. Martinson, R. C. Smith, X. Yuan, and D. Rind (2008), Trends in Antarctic sea ice retreat and advance and their relation to ENSO and Southern Annular Mode variability, *J. Clim*, in press.

Thompson, D. W. J., and S. Solomon (2002), Interpretation of recent Southern Hemisphere climate change, *Science*, *296*(5569), 895–899.

Thompson, D. W. J., J. M. Wallace, and G. C. Hegeri (2000), Annular modes in extra-tropical circulation, Part II: Trends, *J. Clim.*, *13*, 1000–1016.

Timmermann, R., H. Goosse, G. Madec, T. Fichefet, C. Ethe, and V. Dulière (2005), On the representation of high latitude processes in the ORCA-LIM global coupled sea ice-ocean model, *Ocean Modell.*, *8*(1–2), 175–201, doi:10.1016/j.ocemod.2003.12.009.

Turner, J., S. A. Harangozo, G. J. Marshall, J. C. King, and S. R. Colwell (2002), Anomalous atmospheric circulation over the Weddell Sea, Antarctica, during the austral summer of 2001/02 resulting in extreme sea-ice conditions, *Geophys. Res. Lett.*, *29*(24), 2160, doi:10.1029/2002GL015565.

Turner, J., S. A. Harangozo, J. C. King, W. Connolley, T. Lachlan-Cope, and G. J. Marshall (2003), An exceptional winter sea-ice retreat/advance in the Bellingshausen Sea, Antarctica, *Atmos. Ocean*, *41*, 171–185.

Uppala, S. M., et al. (2005), The ERA-40 re-analysis, *Q. J. R. Meteorol. Soc.*, *131*, 2961–3012, doi:10.1256/qj.04.176.

van den Broeke, M. (2000), On the interpretation of Antarctic temperature trends, *J. Clim.*, *13*, 3885–3889.

van Loon, H., and R. L. Jenne (1972), The zonal harmonic standing waves in the Southern Hemisphere, *J. Geophys. Res.*, *77*, 992–1003.

Vaughan, D. G., G. J. Marshall, W. M. Connolley, C. Parkinson, R. Mulvaney, D. A. Hodgson, J. C. King, C. J. Pudsey, and J. Turner (2003), Recent rapid regional climate warming on the Antarctic Peninsula, *Clim. Change*, *60*, 243–274.

Vera, C. S., G. E. Silvestri, V. R. Barros, and A. F. Carril (2004), Differences in El Niño response over the Southern Hemisphere, *J. Clim.*, *17*, 1741–1753.

Weatherly, J. W., J. E. Walsh, and H. J. Zwally (1991), Antarctic sea ice variations and seasonal air temperature relationships, *J. Geophys. Res.*, *96*, 15,119–15,130.

Worby, A. P., R. A. Massom, I. Allison, V. I. Lytle, and P. Heil (1998), East Antarctic sea ice: A review of its structure, properties and drift, in *Antarctic Sea Ice Physical Processes, Interactions and Variability*, *Antarct. Res. Ser.*, vol. 74, edited by M. O. Jeffries, pp. 41–68, AGU, Washington, D. C.

Yuan, X. J., and D. G. Martinson (2001), The Antarctic Dipole and its predictability, *Geophys. Res. Lett.*, *28*, 3609–3612.

Zwally, H. J., J. C. Comiso, C. L. Parkinson, D. J. Cavalieri, and P. Gloersen (2002), Variability of Antarctic sea ice 1979–1998, *J. Geophys. Res.*, *107*(C5), 3041, doi:10.1029/2000JC000733.

N. Adams, Australian Bureau of Meteorology and Antarctic Climate and Ecosystems Cooperative Research Centre (ACE CRC), Private Bag 80, Hobart, Tas 7001, Australia.

C. Fowler, Colorado Center for Astrodynamics Research, University of Colorado, Boulder, CO 80309-0431, USA.

S. A. Harangozo, British Antarctic Survey, Natural Environment Research Council, Madingley Road, High Cross, Cambridge CB3 0ET, UK.

W. Lefebvre, Institut d'Astronomie et de Géophysique Georges Lemaître, Université Catholique de Louvain, Chemin du Cyclotron 2, Louvain-la-Neuve, B-1348 Ottignies-Louvain-la-Neuve, Belgium.

R. A. Massom, Australian Antarctic Division and Antarctic Climate and Ecosystems Cooperative Research Center (ACE CRC), Private Bag 80, University of Tasmania, Hobart, Tas 7001, Australia. (r.massom@acecrc.org.au)

M. J. Pook, CSIRO Division of Marine and Atmospheric Research, Hobart, Tas 7001, Australia.

T. A. Scambos, National Snow and Ice Data Center, University of Colorado, CIRES Campus Box 449, Boulder, CO 80309-0449, USA.

S. E. Stammerjohn, Lamont-Doherty Earth Observatory, Columbia University, Palisades, NY 10964, USA.